

US Army Corps
of Engineers
Detroit District

Milwaukee South Shore Breakwater

Rehabilitation Feasibility Study

May 2001

Milwaukee County
Department of Public Works



DEPARTMENT OF THE ARMY
DETROIT DISTRICT, CORPS OF ENGINEERS
BOX 1027
DETROIT, MICHIGAN 48231-1027

June 29, 2001

IN REPLY REFER TO:

Planning, Programs & Project Management Division
Planning Branch

Mr. Gregory G. High, P.E.
Department of Public Works
Milwaukee County
Courthouse Annex, Room 303
907 North 10th Street
Milwaukee, Wisconsin 53233

Dear Mr. High:

This correspondence is in response to your June 8, 2001, review comments on the final Planning Assistance to States study report entitled, "Milwaukee South Shore Breakwater Rehabilitation Feasibility Study". The purpose of the study was to seek planning assistance to eliminate the current navigation hazard and possible shoreline erosion problems caused by the deterioration of the offshore breakwater.

Enclosed for your use and information is five copies of the final study report which was revised to address your previously noted comments. If you have any other questions relating to the content of the final study report, please contact me at 313-226-6773 or Mr. Charles Uhlarik, program manager, Planning Assistance to States, at 313-226-6753.

Sincerely,

for Joseph R. Wanielista, P.E.
Chief, Planning Branch,
Planning, Programs & Project
Management Division

Enclosure

MILWAUKEE SOUTH SHORE BREAKWATER Rehabilitation Feasibility Study

1.0 INTRODUCTION

1.1 Project Description:

The project area consists of approximately 7,600 feet of an existing offshore-segmented rubblemound breakwater along the Lake Michigan coastline in Milwaukee County, Wisconsin. The breakwater extends from South Shore Park to the south property line of Bay View Park, as shown in Figure 1. Facilities within the project area include South Shore Park and Bay View Park (both of which have beaches), the South Shore Yacht Club, the South Shore Pavilion, a public bicycle path, the Texas Avenue water intake pump station, and several groins.

The Milwaukee County Department of Public Works requested planning assistance from the Army Corps of Engineers, Detroit District, to eliminate the current navigation hazard and possible shoreline erosion problems caused by the deterioration of the offshore breakwater.

1.2 Authority and Acknowledgements:

The source of authority for this study is Section 22 of the Water Resources Development Act (WRDA) of 1974 (Public Law 93-251), as amended. This act assists local or state entities in the preparation of plans for the development, utilization and conservation of water and water related resources.

1.3 Background Information:

The shoreline in the project area has been the subject of many shoreline studies.

- Section 14 of the Flood Control Act of 1946 (PL79-526): A request was made by the Deputy Director of Parks, Recreation, and Culture, Milwaukee County, on 25 November 1985, to provide assistance concerning the beach erosion problem in South Shore Park and Bay View Park. A 340-foot temporary shoreline revetment was constructed by the county to protect the South Shore pavilion. The revetment consists of 1,080 cubic yards of 1 to 3 ton armor stone and 2,670 cubic yards of 1 to 500 pound concrete rubble and limestone rock as an underlayer. The design analysis report, dated 8 March 1991, noted that the temporary revetment had ceased or slowed the erosion considerably, and recommended incorporating and replacing the temporary revetment with a 430-foot revetment.
- "Conceptual Design for Shoreline Stabilization", Foth & Van Dyke, 1990 – Prepared for Milwaukee County. Foth & Van Dyke recommended constructing rock revetments with slope stabilization and drainage features, as required.
- "Lake Michigan Shoreline Recession and Bluff Stability in Southeastern Wisconsin: 1995", Southeastern Wisconsin Regional Planning Commission (SWRPC). Study of shoreline erosion and bluff stability conditions along the Lake Michigan Shoreline in 1995, and a

comparative analysis to conditions during the last study in 1987. The findings showed that the bluffs in the project area had become more stable since 1987, and were not in danger of failing, assuming that the breakwater continued to protect the shoreline.

2.0 EXISTING SITE CONDITIONS

2.1 Available Data

The Corps of Engineers, Detroit District collected the following data during the feasibility study:

- Scanning Hydrographic Operational Airborne Lidar Survey (SHOALS), 1998. Data not suitable for modeling, as discussed in Appendix 1.
- Coastal Hydrodynamic Analysis, December 2000, provided as Appendix 1
- Hydrographic survey of the breakwater in the project area, provided as Enclosure 1. June 1999, Kewaunee Area Office
- Site visit, extensive photos taken of shoreline and breakwater structure, August 1999. Select photos are provided in Appendix 2.

2.2 Offshore segmented breakwater

The project area includes a segmented granite breakwater located approximately 1,200 feet offshore. The breakwater was constructed in the 1920s, and was most likely constructed by end dumping the granite from a barge, and allowing it to fall at its angle of repose. Existing stone size is estimated at 7 to 12 tons.

There are several areas of the breakwater that have deteriorated to levels below the high water mark. During high water levels, these areas may appear to be entrances to the harbor, thereby posing a navigational safety hazard. There are also concerns that the deteriorated breakwater is not protecting the shoreline adequately. Several existing cross sections are shown in Figures 2a and 2b.

2.2.1 Breakwater - Cause of Deterioration

It is necessary to determine the cause of deterioration of the breakwater before determining the appropriate rehabilitation method. Most deterioration occurs from one (or a combination) of four actions: 1) Ice forces; 2) Wave forces; 3) Settlement of structure; and 4) Inferior stone. This section explores the applicability of each action.

Ice can exert pressure on a breakwater structure in a variety of ways. Floating ice sheets can inflict damage by direct impact, deteriorating the condition of the breakwater. Expansion of entrapped water within the breakwater will exert pressure on the structure. Ice formations can remove material from the structure due to a 'plucking action', known as ice rafting. Deterioration due to ice forces is very likely at this site. Although the stone is of high quality, the construction method, 'end dumping', provides very little interlocking of stones. This encourages further deterioration due to expansion and direct forces, allowing ice rafts to easily 'pluck' away loose stones.

Wave forces can cause damage to breakwater structures by repeated impact to the structure. Excessive wave force can dislodge stone, and cause disbursement along the structure. The rounding of the stone edges is an indication of such forces. As shown in Photo 8, the edges of the South Shore breakwater do not show signs of deterioration due to wave action.

Two types of settlement may contribute to the deterioration of a breakwater. 1) Settlement due to subsoils, and 2) settlement of breakwater stone. If a breakwater is situated on soils not capable on supporting the loads exerted by the structure, settlement can occur. Although soil borings were not taken during this study, breakwaters in the vicinity have not experienced excessive settlement. Some settlement of the stones themselves likely occurred, due to the random placement during construction. However, the remaining stone appears to have settled into a tight formation, and no continued settlement is likely.

Inferior stone supply is another cause of breakwater deterioration. Low quality stone can quickly degrade and cause failure of the structure. This does not appear to be the case at South Shore breakwater, as the remaining stone appears to be excellent quality.

In summary, the most probable factor in the deterioration of the breakwater is the method of rock placement, which did not provide significant interlocking, and was therefore susceptible to ice rafting and wave forces. The remaining breakwater appears to have settled in to a tight configuration, and further settlement is unlikely.

2.3. Shoreline Condition

The beach at the South Shore Park in the northern portion of the project area was estimated at widths up to 200 feet in 1995. The southern tip is currently protected by concrete rubble, and has little to no beach remaining.

The shoreline within the project contains bluffs, ranging in height from 25 to 60 feet. The materials appear to be sandy silt overlain by till material. A majority of the bluffs located in the project area are primarily covered with vegetation, and do not appear to have any signs of active erosion. The southernmost bluffs also are vegetated, but signs of active gullying were found during the August 1999 site visit. (See Appendix 2, photos 17 & 18).

2.3.1 Shoreline – Cause of Deterioration

Lake Michigan experienced record high water levels during late 1986 and 1987. It is likely that these bluffs became steeper during this period, after the toe was removed by wave action. This undercutting action would then leave the bluffs in an unstable condition, leading to the slumping or sliding of the bluff face. Due to the cohesive properties of the bluffs stiff clays, the slope may not quickly react to toe erosion.

As mentioned earlier, gullying was found in the southern portions of the project area. Gullying is the result of surface water runoff flowing over the top of the bluff, and over the slope face itself. The runoff detaches soil particles from the bluff face and transports them down the slope.

The bluffs in the project area appear to have reached a stable slope in areas not affected by gully erosion. Surface runoff and drainage control is necessary to control bluff recession in the southern area. A study of the contributing point and non-point sources should be conducted to determine suitable control measures. However, this is outside of the scope of this study.

3.0 DESIGN DEVELOPMENT

3.1 Design Assumptions

After establishing these basic criteria the project team developed technical assumptions needed to develop conceptual designs. These assumptions will require verification in the final design process. They include:

- A. Site specific subsurface conditions are relatively unknown. A hydrographic survey was conducted along the breakwater, but no geophysical surveys or soil samples were taken during the feasibility study.
- B. The county does not have any maintenance or improvements scheduled prior to the completion of the feasibility report. Therefore, site conditions are not expected to change between the date of request and completion of feasibility study.
- C. Any necessary real estate easements and rights of way will be acquired prior to project implementation.
- D. Drainage of storm water runoff, groundwater, and springs in the project area will require special consideration and will not be a part of this study.

3.2 Shoreline Protection Concepts - Alternative Evaluation

Several on-shore and off-shore methods are available to protect the shoreline and eliminate potential navigational hazards posed by the current project conditions. The four alternatives discussed in this feasibility study were chosen with consideration to the intended use of the project area and cost. The alternatives include; 1) Rehabilitate the existing breakwater to original elevations, 2) Remove existing breakwater structure and provide on-shore protection; 3) convert the segmented breakwater to a continuous breakwater; and 4) demarcation of safety hazards.

3.2.1 Alternative One – Rehabilitate existing breakwater structure (Recommended Option)

The existing stone has been dispersed in many locations along the South Shore Breakwater, reducing approximately 1200 lineal feet to elevations below high water levels along the middle segment of the breakwater. Concern has been raised that gaps resulting from subsidence of the structure may allow a large quantity of wave energy to pass the structure and reach the beach and bluff. The hydrodynamic study determined the breakwater in its present condition to be

adequate in preventing most wave energy from passing the breakwater. The structure will cause storm waves to break as they pass over the structure, resulting in the loss of most wave energy (See Appendix 1).

Even if further degradation to the structure does not occur, a navigational hazard still exists. By restoring the top height to an elevation 583.8 feet IGLD 1955 (7.0 feet above LWD), and restoring side slopes to 1V: 2H, both concerns would be addressed. The 'middle segment' is the recommended area of repair as shown on the December 2000 hydrographic survey, provided as Enclosure 1. The southern segment of the breakwater appears to be in fair condition, and is not at this time recommended for repair.

The breakwater elevation as recommended in this study assumes that at times erosion of the beach and bluff will occur. These bluffs were formed more than 10,000 years ago when the glaciers retreated. Since their creation, these bluffs have been eroding. To halt this erosion would require the removal of all openings in the county breakwater, in addition to sealing the southern end. Furthermore, the height of the structure would need to be increased to prevent overtopping of all waves. Such a massive structure would be considerably more expensive than the proposed plan.

Several existing cross sections are shown in Figures 2a and 2b. The elevations shown on the cross sections are taken from the December 2000 hydrographic survey (Enclosure 1). The remaining stone at the South Shore Breakwater has settled into a relatively tight configuration. The careful placement and sizing of stones to fill existing voids is more efficient than attempting to reconstruct a complete armor layer. The slope of the existing stone ranges from approximately 1V: 3H to 1V:4H. This is considerably less steep than the required slope of 1V:2H. Existing stone can be reused where recoverable and if it meets the required size and quality criteria.

Stone sizing was computed to establish a minimum size for areas requiring more than the filling of voids. Before the Hudson equation can be used to determine the approximate stone size, a wave height must be established. A complete wave analysis was outside of the scope of this feasibility study. A range of design wave heights was estimated at 7.8 to 16.4 feet. A 1997 study¹ determined the design wave height at the South Shore Yacht Club to be 14.3 feet. This height yielded a stone size of 6 to 12 ton stone, which is used for cost estimating purposes. Before proceeding to the design phase, a formal wave analysis should be completed.

3.2.2 Alternative Two – Remove the breakwater structure, provide shoreline revetment

This alternative provides onshore protection via a revetment, in place of the existing offshore breakwater structure. Weights of rock for the bluff and lakebed protection have been assigned on the basis of experience with similar lakeshore construction projects involving similar wave and wind forces. An estimated 5700 feet of shoreline would require protection, from the storm sewer outflow structure located approximately 1000 feet north of the power plant and extending north to the Texas Avenue Pump Station located at Texas Avenue. This is a preliminary estimate, and would require further study of existing shoreline conditions.

¹ Milwaukee Harbor, WI Dredged Material Management Plan Study, USACE, Detroit District, January 1997.

For the purpose of cost estimating, the proposed revetment section assumes two conditions that are conservative at this stage and will have to be considered more thoroughly in final design. The quality and/or density of the soils underlying the proposed revetments are assumed to require removal and replacement, therefore full depth excavation is anticipated. The second assumption is that any revetment installation would provide toe scour protection at elevation 576.0 feet (IGLD 1955) regardless of the topography and lake level. This assumption is prudent because even in the present beach, future high water levels may displace the overlying sands and expose the revetment toe to undermining. Because of these assumptions, a full depth excavation is proposed for the construction of the beach area revetment. The excavated fill will be backfilled over the toe of the revetment to provide the beach appearance after construction is complete (See Figure 3).

As discussed earlier, the existing breakwater is adequately protecting the shoreline. Removing the breakwater structure would allow significant wave energy to reach the beach and bluff. Construction of revetments along the bluffs in place of offshore protection would allow the beach to be eroded by wave forces. Any sediments that have deposited along the land side of the breakwater will also erode. Furthermore, construction of a stone revetment would limit access to the shore.

3.2.3 Alternative Three – Convert segmented breakwater to a continuous breakwater.

The existing South Shore breakwater has two designed ‘gaps’ to allow for vessel passage. In addition, several areas along the breakwater have deteriorated. This alternative involves filling these gaps and areas of deterioration in an effort to control shoreline erosion.

A hydrodynamic analysis of this alternative (Appendix 1) suggested that closing the gaps would provide minimal protection to the beach and bluff. It is also likely to cause stagnation of the water behind the breakwater, possibly resulting in water quality and aesthetic problems. Moreover, vessels would be required to travel a greater distance before reaching the sheltered water behind the structure. It is also likely that a channel would have to be designated and maintained in these shallow waters if this option were implemented.

3.2.4 Alternative Four – Demarcation (No Structural Action)

This alternative explores the results if no structural action is taken. The deteriorated portions of the breakwater may pose a navigational safety hazard to boaters during high water periods, when deteriorated areas may be mistaken for entrances. If no action is taken, buoys and sufficient demarcation of the partially submerged structure may be needed to warn mariners of the potential danger. In addition, a Notice to Mariners should be issued describing the potential hazard. The cost estimate assumes that the buoys would be spaced every 30 feet over the estimated 1200 lineal feet of deteriorated breakwater.

While the breakwater in its current condition provides adequate wave protection to the shoreline, this is likely to be only a temporary solution. The breakwater is likely to further deteriorate over time, potentially reducing the protection to the shoreline. This alternative would require monitoring of the existing breakwater to determine if deterioration is occurring. Monitoring costs are not included in the attached estimate.

4.0 RECOMMENDED ALTERNATIVE

Table 1 summarizes the estimated costs for each alternative, while a more detailed estimate is provided as Appendix 3.

TABLE 1: ESTIMATED COST

Alternative	Estimated Cost
Alt. One – Rehab existing breakwater	\$2,054,400.00 ¹
Alt. Two – Shoreline Revetment, remove breakwater	\$2,006,400.00
Alt. Three – Create continuous breakwater	\$2,486,400.00 ¹
Alt. Four – Demarcation	\$44,200.00

1. Alternatives One and Three assume no repair to the southern segment of the breakwater. To restore the southern section to +7.0, costs for Alternatives one and three would increase by approximately \$625,000 (13,000 tons of additional stone).

The hydrodynamic analysis found that neither Alternative Two nor Alternative Three provided increased protection to the beach, and are therefore undesirable. Alternative Four (demarcation) addresses the navigational safety hazard at a relatively low cost. Hydrodynamic analysis shows that the existing breakwater is protecting the shoreline from wave erosion. However, ice rafts and/or wave action may deteriorate the breakwater further, reducing the protection to the shoreline.

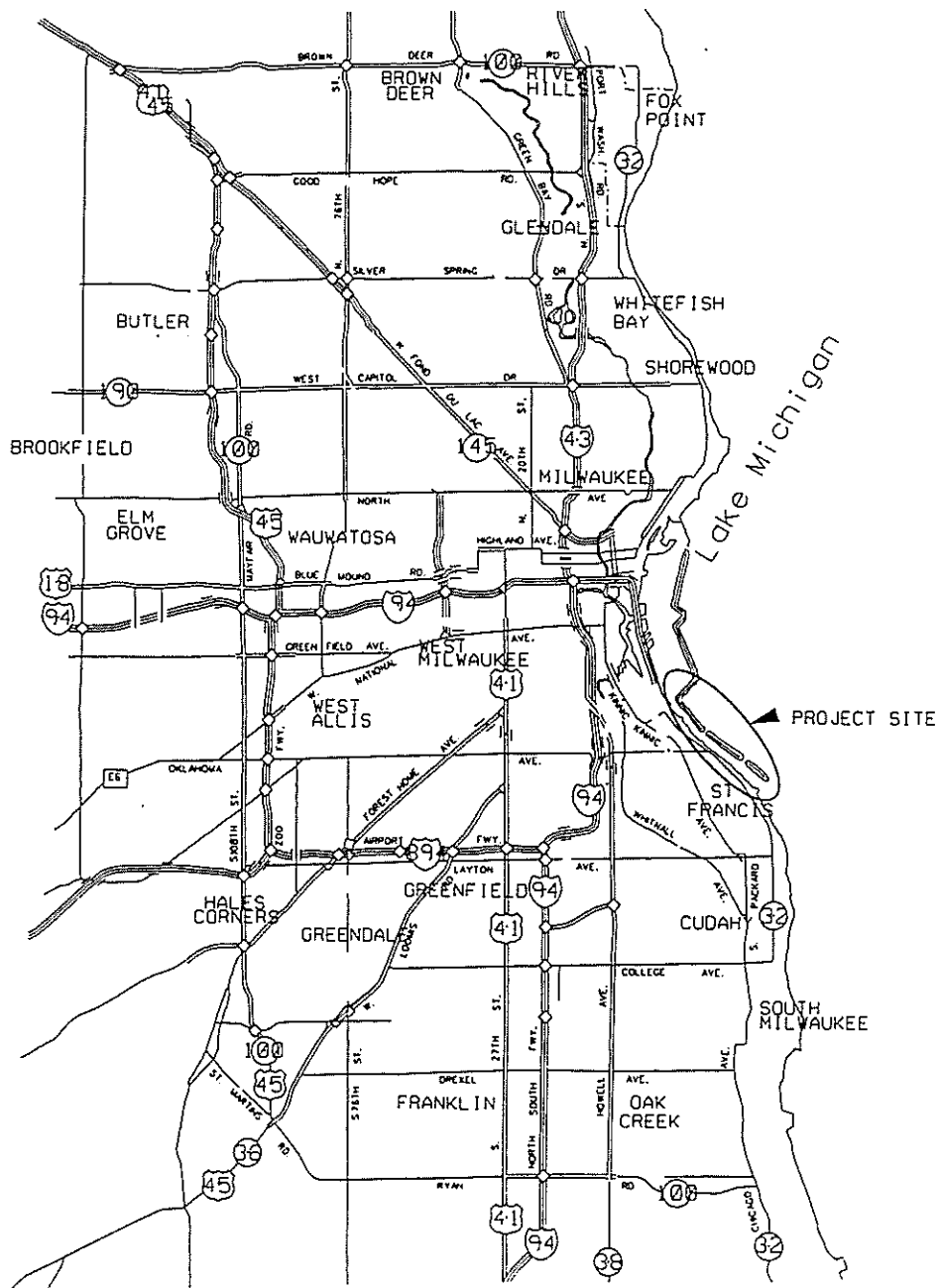
Alternative One is the recommended alternative. It addresses the navigational safety hazard, while interlocking and chinking of the new stone would deter further deterioration of the breakwater. Alternative One is consistent or superior to similar sites around the Great Lakes. To completely stop erosion of the bluff would require the construction of a massive structure, similar to the coastal defenses constructed at the Chicago waterfront. These structures cost in excess of \$300 million to construct. Such a high cost is not likely justified in protecting a public beach and park. Another method of increasing protection against bluff erosion, especially in a high water level condition, would be to install a combination of the recommended breakwater restoration in Alternative #1 and areas of shoreline revetment discussed in Alternative #2. The location of the shoreline revetment would be dependent on the outcome of further coastal engineering study and analysis and taking into account the planning and design of future shoreline improvements such as beach, hiking trail and bike trail development. This added protection would require a significant cost increase over the recommended breakwater restoration plan.

CONCLUSION

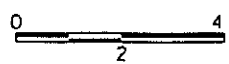
The recommended alternative, Alternative One, consists of restoring deteriorated portions of the South Shore breakwater to 584 feet above mean sea level, I.G.L.D. 1955. Restoration includes placement of 6 to 10 ton stone to the required elevation at a 1V: 2H slope. Existing stone that has fallen from the structure may be reused if suitable. It should be noted that stone sizing was based on an assumed design wave height, and will need to be analyzed further during the design

phase. Specialized placement of stone is recommended to increase interlocking of stone, and minimize deterioration due to ice rafting wave action.

This feasibility study determined that current erosion along the shore is limited to bluff erosion. Groundwater and surface water runoff are forming gullies, which are actively eroding the bluffs. A study of the local hydrology contributing to the gully formation is outside the scope of this study, but is strongly recommended to control bluff erosion.



VICINITY MAP



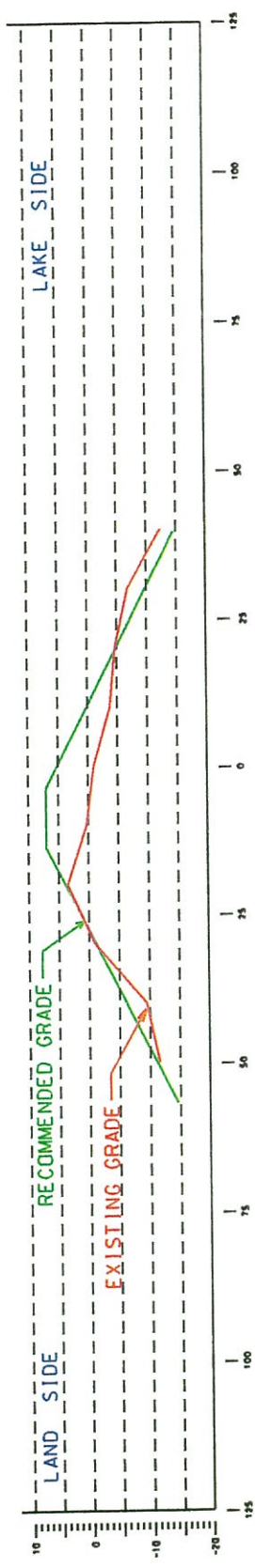
SCALE IN MILES

FIGURE 1

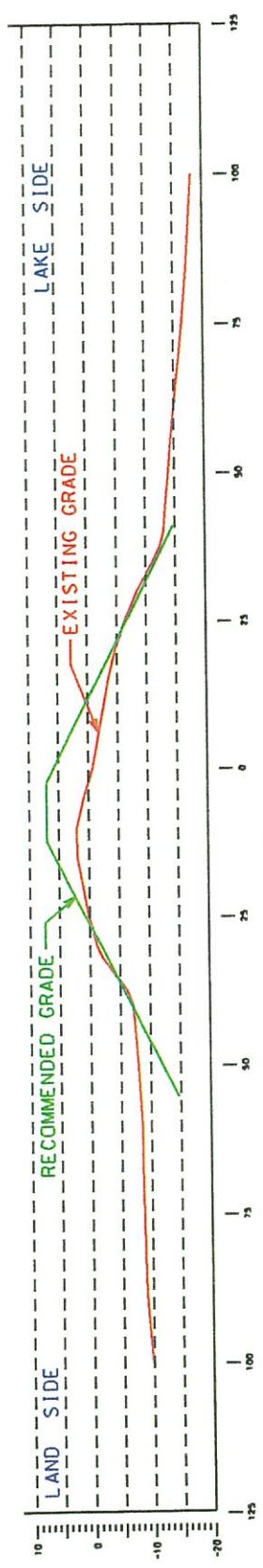
MILWAUKEE HARBOR
 WISCONSIN
 SOUTH SHORE
 LAKE MICHIGAN

VICINITY MAP

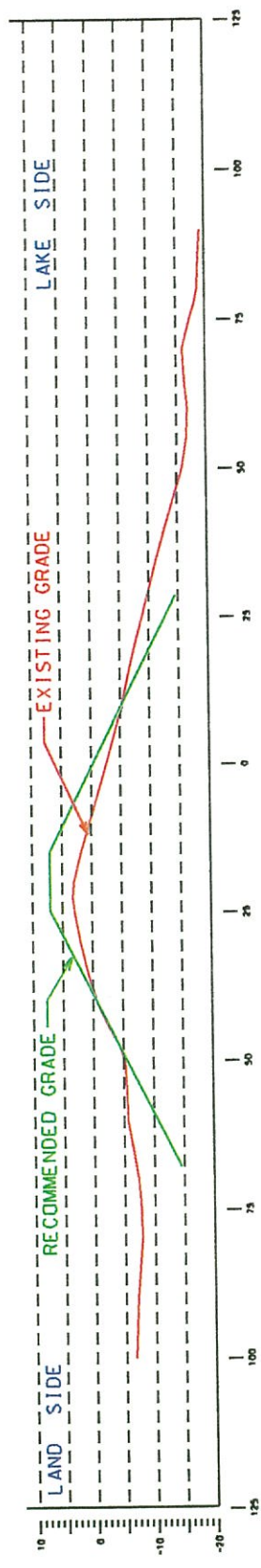
U.S. ARMY ENGINEER DISTRICT, DETROIT
 JUNE 21 1999



SECTION A - A



SECTION B - B



SECTION C - C

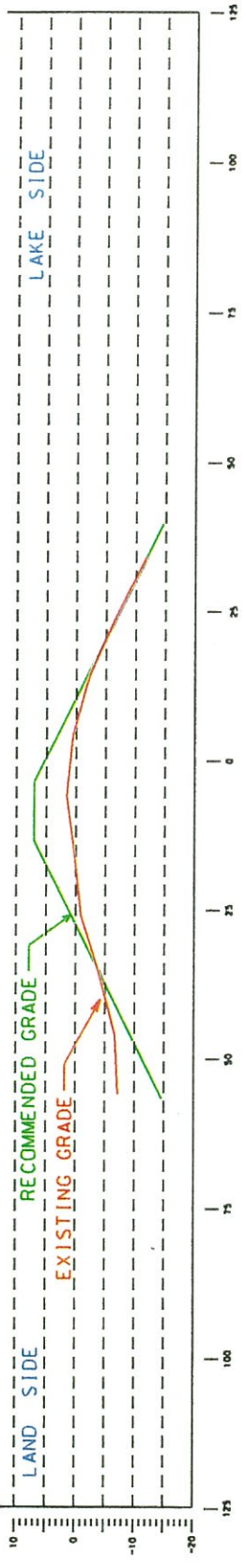
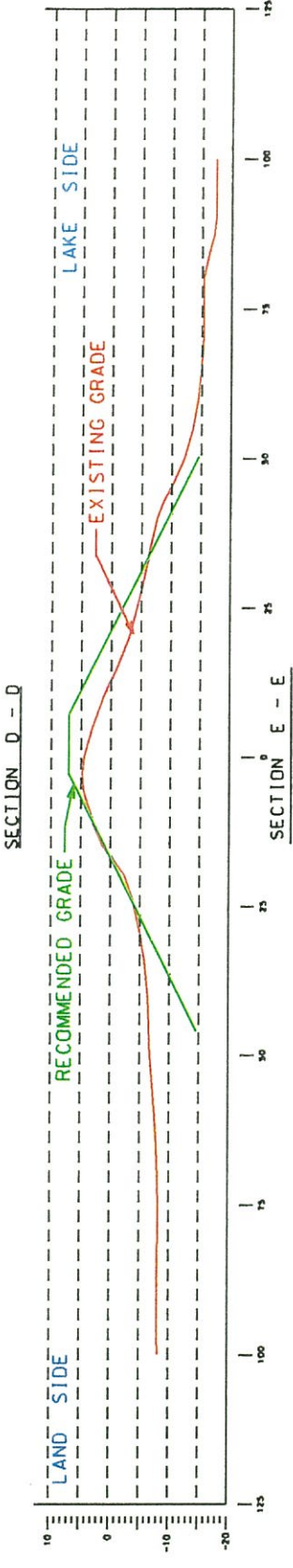
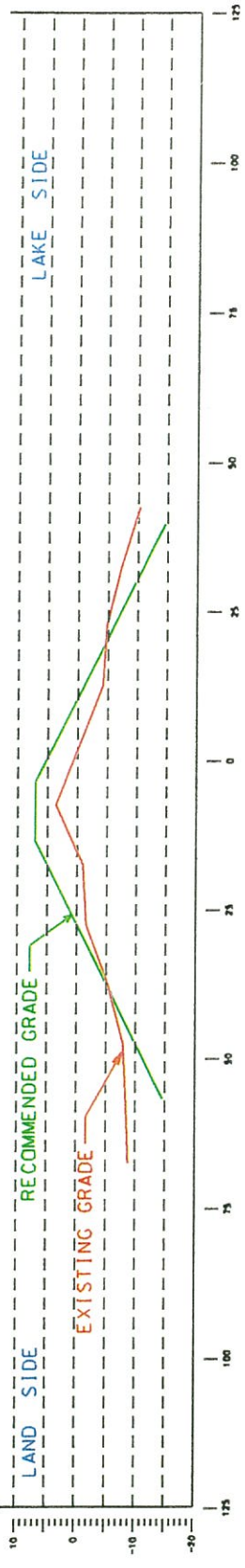
ELEVATIONS SHOWN ARE TAKEN FROM THE JUNE 1999 HYDROGRAPHIC SURVEY.
 ALL ELEVATIONS ARE IN FEET AND REFERENCED TO THE LOW WATER DATUM
 ELEVATION, 576.8 FEET ABOVE MEAN SEA LEVEL, I.G.L.D. 1955.

SCALE 1" = 30'-0"



FIGURE 2A

MILWAUKEE HARBOR,
 WISCONSIN
 SOUTH SHORE BREAKWATER
 EXISTING AND PROPOSED
 CROSS SECTIONS
 U.S. ARMY ENGINEER DISTRICT, DETROIT
 SEPTEMBER, 2000

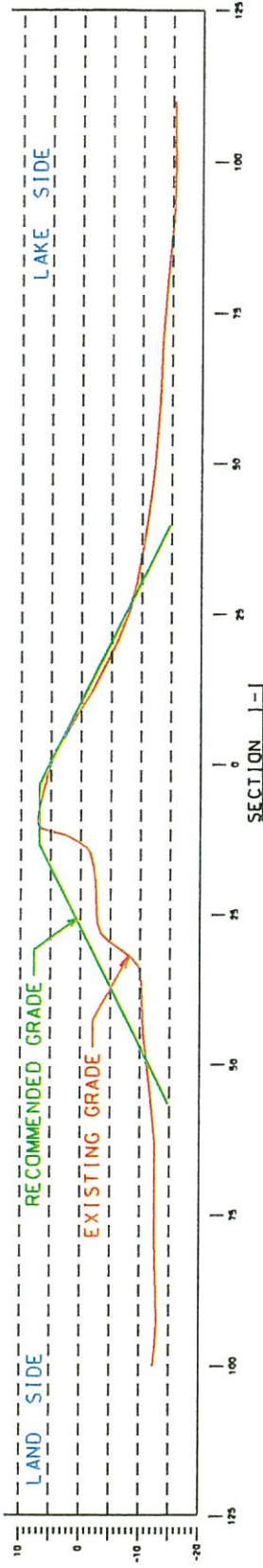
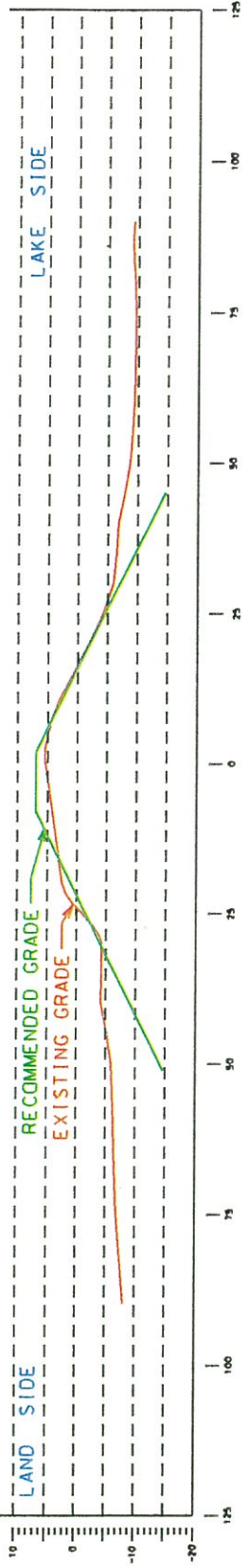
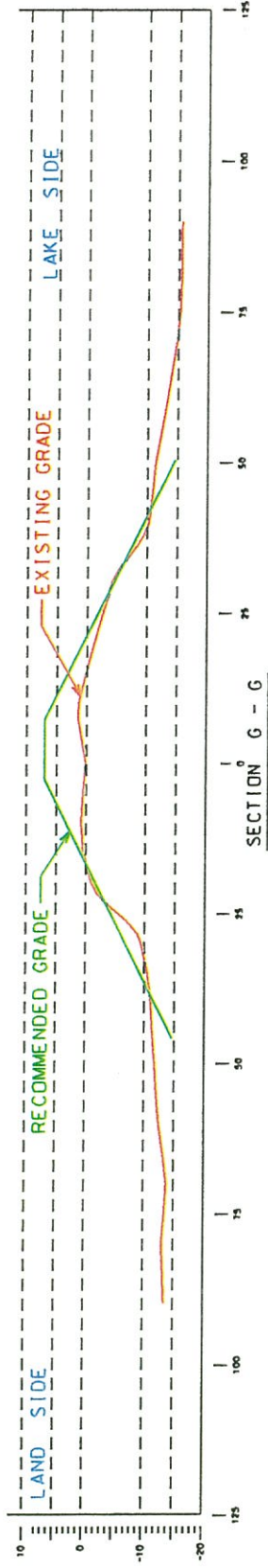


ELEVATIONS SHOWN ARE TAKEN FROM THE JUNE 1999 HYDROGRAPHIC SURVEY.
 ALL ELEVATIONS ARE IN FEET AND REFERENCED TO THE LOW WATER DATUM
 ELEVATION, 576.8 FEET ABOVE MEAN SEA LEVEL, I.G.L.D. 1955.

SCALE 1" = 30'-0"

FIGURE 2B

MILWAUKEE HARBOR,
 WISCONSIN
 SOUTH SHORE BREAKWATER
 EXISTING AND PROPOSED
 CROSS SECTIONS
 U.S. ARMY ENGINEER DISTRICT, DETROIT
 SEPTEMBER, 2000

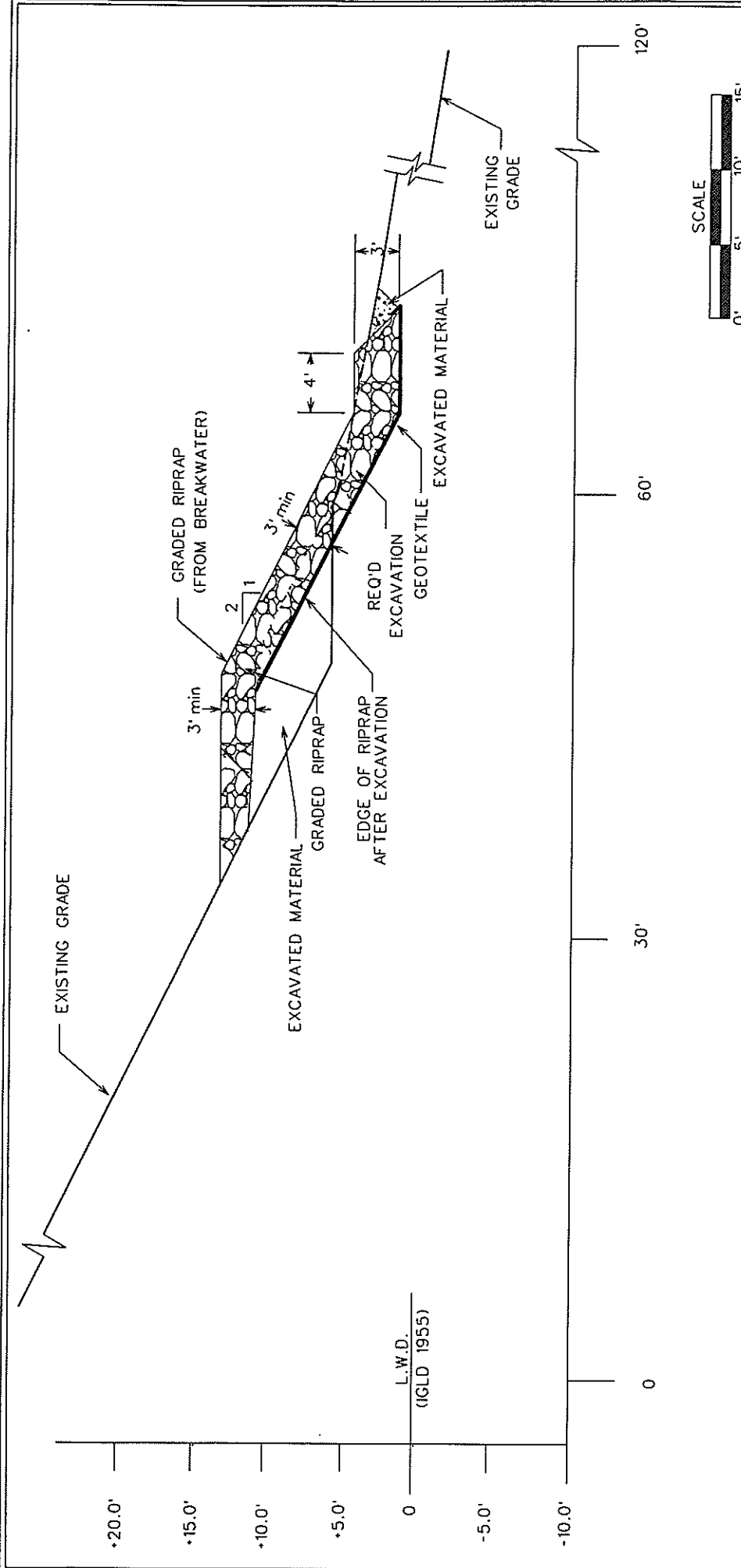


ELEVATIONS SHOWN ARE TAKEN FROM THE JUNE 1999 HYDROGRAPHIC SURVEY.
 ALL ELEVATIONS ARE IN FEET AND REFERENCED TO THE LOW WATER DATUM
 ELEVATION, 576.8 FEET ABOVE MEAN SEA LEVEL, I.G.L.D. 1955.

SCALE 1" = 30'-0"

FIGURE 2C

MILWAUKEE HARBOR,
 WISCONSIN
 SOUTH SHORE BREAKWATER
 EXISTING AND PROPOSED
 CROSS SECTIONS
 U.S. ARMY ENGINEER DISTRICT, DETROIT
 SEPTEMBER, 2000



MILWAUKEE HARBOR
 WISCONSIN
 SOUTH SHORE
 LAKE MICHIGAN
 ALTERNATIVE TWO
 REVERTMENT X-SECTION
 U.S. ARMY ENGINEER DISTRICT, DETROIT
 JANUARY 2001

FIGURE 3

APPENDIX 1

**COASTAL HYDRODYNAMIC ANALYSIS
MILWAUKEE BREAKWATER**

**U.S. Army Corps of Engineers
Detroit District
Great Lakes Hydraulics and Hydrology Office**

December 2000

Introduction

The southern 7632 ft of the Milwaukee Breakwater consists of a segmented offshore breakwater (Figure A-1). Two openings, the north and south entrance, were designed into this structure and constructed between 1918 and 1931. Presently, the breakwater has subsided causing several locations along the structure to be submerged during normal to high water regimes. In its current condition, the structure poses a navigation hazard. Furthermore, the bluff in the lee of the breakwater is eroding. The bluffs along Bayview Park are failing due to a combination of wave and groundwater forces. The relative degree to which waves or groundwater causes bluff failure is discussed. Several options have been presented in this report to address the current navigation hazard. In general, the structural alternatives are: 1) rehabilitate the structure to the original height, 2) remove the structure and place the breakwater stone on the toe of the bluff as a revetment and 3) close gaps in the breakwater. The non-structural alternative consisted of providing buoys and sufficient demarcation of the partially submerged structure to warn mariners of the potential danger.

Bluff Composition and Failure

Based on the findings in SWRPC, et al., 1997 the bluffs are composed primarily of till underlain by sand and silt. The bluff height varies from 25 to 35 feet. Based on a site visit in August 1999, it was observed that the bluff face was mostly vegetated. However, several locations were identified as actively failing. All of these sites were failing due to groundwater seepage and gulying from overland flow. During the site visit, no evidence was observed that waves have recently reached the toe of the bluff. It is likely that these bluffs were steepened during the last high-water period, in 1986. The steepening occurred when material was removed from the toe by wave action. Once the lake levels receded, the top of the bluff began to fail due to groundwater forces and overland flow, in an attempt to achieve a stable slope. It is likely that the bluff failures observed today are the results of an oversteepening that occurred a number of years ago. A bluff stability analysis was performed by SWRPC et al. (1997). The analysis indicated an increase in bluff safety factor between the bluff profile in 1987 and that in 1995. Specifically, in 1987, the safety factor was calculated to range from 0.81 to 0.99; while in 1995 the safety factor was calculated to range from 0.9 to 1.01. These results, along with observations in the referenced report, indicate that the bluff is becoming considerably less steep. Two recommendations are suggested to reduce the ongoing failure of the bluff. First, redirecting runoff away from the bluff may reduce the erosion caused by surface runoff. Second, dewatering the aquifers that feed water to the bluff face may reduce failure due to groundwater. The final component to be addressed in the failure of these bluffs pertains to the amount of wave energy allowed to reach the toe of the bluff. The remainder of this report addresses the structural alternatives to minimize wave energy reaching the bluff.

Survey/Bathymetric Data

Bathymetric data from three sources was obtained for use in these hydraulic modeling efforts. In 1998 a Scanning Hydrographic Operational Airborne Lidar Survey (SHOALS) was conducted for the Federal portion of the Milwaukee breakwater, which continued south of the federal structure to include the 6 miles of structure owned by Milwaukee County. A successful lidar survey requires minimal turbidity in the water column. Storms on Lake Michigan during this survey caused increased turbidity, thus preventing the survey lasers from sufficiently penetrating the water. The SHOALS data was examined and determined to be of poor quality. It was concluded that this data should not be used for modeling purposes. The extent of SHOALS coverage is shown in Figure A-2. Note that good-quality data could only be collected in the shallow water near the breakwater.

A conventional hydrographic survey was performed to collect the necessary bathymetric data. The survey lines for the conventional survey are shown on Figure A-3. This bathymetry was supplemented with NOS data to produce sufficient bathymetric resolution. The spatial extent of NOS data is shown on Figure A-4. The survey data sets for all three sources are included on the enclosed CD.

Coastal Modeling

Two coastal models were applied to quantify the effects of the above alternatives on the wave climate in the lee of the breakwater. A wave-growth/wave-transformation model, STWAVE, was used to define the offshore wave climate, while a wave-agitation model, CGWAVE, was used to describe the wave climate between the breakwater and the shore. A direct quantification of erosion or bluff recession is not possible; however, by comparing the wave energies in the lee of the structure, the alternatives can be compared as to their potential to erode the beach and bluff.

STWAVE

STWAVE (STeady-state spectral WAVE model) (Resio 1987, 1988a, 1988b; Davis 1992) is a phase-averaged spectral wave model. This approach uses a steady-state finite-difference model based on the wave action balance equation. A complete description of STWAVE can be found in Smith et al., 1998.

Model Capabilities

The purpose of applying nearshore wave transformation models is to describe quantitatively the change in wave parameters (wave height, period, direction, and spectral shape) between the offshore and the nearshore (typically depths of 20 m or less). In relatively deep water, the wave field is fairly homogeneous on the scale of kilometers; but in the nearshore, where waves are strongly influenced by variations in bathymetry, water level, and current, wave parameters may vary significantly on the scale of tens of meters. Offshore wave information is typically available from a wave

gauge or a global- or regional-scale wave hindcast or forecast. Nearshore wave information is required for the design of almost all coastal engineering projects. Waves drive sediment transport and nearshore currents, induce wave setup and runup, excite harbor oscillations, or impact coastal structures. The longshore and cross-shore gradients in wave height and direction can be as important as the magnitude of these parameters for some coastal design problems.

STWAVE simulates depth-induced wave refraction and shoaling, current-induced refraction and shoaling, depth- and steepness-induced wave breaking, diffraction, wave growth because of wind input, and wave-wave interaction and white capping that redistribute and dissipate energy in a growing wave field.

A wave spectrum is a statistical representation of a wave field. Conceptually, a spectrum is a linear superposition of monochromatic waves. A spectrum describes the distribution of wave energy as a function of frequency (one-dimensional spectrum) or frequency and direction (two-dimensional spectrum). The peak period of the spectrum is the reciprocal of the frequency of the peak of the spectrum. The wave height (significant or zero-moment wave height) is equal to four times the area under the spectrum. STWAVE is based on the assumption that the relative phases of the spectral components are random, and thus phase information is not tracked (i.e., it is a phase-averaged model). In practical applications, wave phase information throughout a model domain is rarely known accurately enough to initiate a phase-resolving model. Typically, wave phase information is only required to resolve wave-height variations near coastal structures for detailed, near-field reflection and diffraction patterns. Thus, for these situations, a phase-resolving model, such as CGWAVE, should be applied.

Model Assumptions

The assumptions made in STWAVE version 2.0 are:

- a. Mild bottom slope and negligible wave reflection. STWAVE is a half-plane model, meaning that wave energy can propagate only from the offshore toward the nearshore (± 87.5 deg from the x axis of the grid, which is typically the approximate shore-normal direction). Waves reflected from the shoreline or from steep bottom features travel in directions outside this half plane and thus are neglected. Forward-scattered waves, e.g., waves reflected off a structure but traveling in the +x direction, are also neglected.
- b. Spatially homogeneous offshore wave conditions. The variation in the wave spectrum along the offshore boundary of a modeling domain is rarely known, and for domains on the order of tens of kilometers, is expected to be small. Thus, the input spectrum in STWAVE is constant along the offshore boundary.
- c. Steady-state waves, currents, and winds. STWAVE is formulated as a steady-state model. A steady-state formulation reduces computation time and is appropriate for wave conditions that vary more slowly than the time it takes for waves to transit the computational grid. For wave generation, the steady-state assumption means that the winds have remained steady sufficiently long for the waves to attain fetch-limited or fully developed conditions (waves are not limited by the duration of the winds).

- d. Linear refraction and shoaling. STWAVE incorporates only linear wave refraction and shoaling, thus does not represent wave asymmetry. Model accuracy is therefore reduced at large Ursell numbers (wave heights are underestimated).
- e. Depth-uniform current. The wave-current interaction in the model is based on a current that is constant through the water column. If strong vertical gradients in current occur, their modification of refraction and shoaling is not represented in the model. For most applications, three-dimensional current fields are not available. At Milwaukee Harbor, wave-current interactions were considered negligible and were not modeled.
- f. Bottom friction is neglected. The significance of bottom friction on wave dissipation has been a topic of debate in wave modeling literature. Bottom friction has often been applied as a tuning coefficient to bring model results into alignment with measurements. Although bottom friction is easy to apply in a wave model, determining the proper friction coefficients is difficult. Also, propagation distances in a nearshore model are relatively short (tens of kilometers), so that the cumulative bottom friction dissipation is small. For these reasons, bottom friction is neglected in STWAVE.

The following sections describe wave propagation and source/sink terms in STWAVE.

Governing Equations

Interaction of waves with currents is considered in a reference frame moving with the current. The wave dispersion relationship is given in the moving reference frame by Jonsson 1990 and others.

Refraction and shoaling

Refraction and shoaling are implemented in STWAVE by applying the conservation of wave action along backward traced wave rays. Rays are traced in a piecewise manner, from one grid column to the next. The two-dimensional wave spectra are set as input along the first grid column (the offshore boundary). For a point on the second grid column, the spectrum is calculated by back tracing a ray for each frequency and direction component of the spectrum. The ray direction, μ , is determined. Only ray directions propagating toward the shore (-87.5 to +87.5 deg) are included. Energy propagating toward the offshore is neglected.

The wave ray is traced back to the previous grid column, and the length of the ray segment DR is calculated. Derivatives of depth and current components normal to the wave orthogonal are estimated (based on the orthogonal direction at column 2) and substituted into Mei's Equation to calculate the wave orthogonal direction at column 1. Then, the wave number, wave and group celerities, and ray angle in the previous column are calculated. The energy is calculated as a weighted average of energy between the two adjacent grid points in the column and the direction bins. The energy density is corrected by a factor that is the ratio of the 5-deg standard angle bandwidth to the width of the back-traced band to account for the different angle increment in the

back-traced ray. The shoaled and refracted wave energy in column 2 is then calculated from the conservation of wave action along a ray.

In a strong opposing current (e.g., ebb currents at an inlet), waves may be blocked by the current. Blocking occurs if there is no solution to the dispersion equation. Or, to state it another way, blocking occurs if the relative wave group celerity is smaller than the magnitude of the opposing current, so wave energy cannot propagate against the current. In deep water, blocking occurs for an opposing current with magnitude greater than one-fourth the deepwater wave celerity without current ($0.25 g T_a / (2B)$, where T_a is the absolute wave period). If blocking occurs, the wave energy is dissipated through breaking.

Diffraction

Diffraction is included in STWAVE in a simple manner through smoothing of wave energy. The model smoothes energy in a given frequency and direction band using the following form

$$E_j(\omega_a, \theta) = 0.55E_j(\omega_a, \theta) + 0.225(E_{j+1}(\omega_a, \theta) + E_{j-1}(\omega_a, \theta)) \quad (1)$$

where E is the energy density in a given frequency and direction band, and the subscript j indicates the grid row index (alongshore position). Equation 1 provides smoothing of strong gradients in wave height that occur in shelter regions, but provides no turning of the waves. This formulation is grid spacing dependent, which is a serious weakness.

Source/sink terms

Surf-Zone Wave Breaking. The wave-breaking criterion applied in the first version of STWAVE was a function of the ratio of wave height to water depth

$$\frac{H_{m0_{max}}}{d} = 0.64 \quad (2)$$

where H_{m0} is the energy-based zero-moment wave height. At an inlet, where waves steepen because of the wave-current interaction, wave breaking is enhanced because of the increased steepening. Smith, Resio, and Vincent (1997) performed laboratory measurements of irregular wave breaking on ebb currents and found that a breaking relationship in the form of the Miche criterion (1951) was simple, robust, and accurate

$$H_{m0_{max}} = 0.1L \tanh kd \quad (3)$$

(see also Battjes 1982 and Battjes and Janssen 1978). Equation 3 is applied in version 2.0 of STWAVE as a maximum limit on the zero-moment wave height. The energy in the spectrum is reduced at each frequency and direction in proportion to the amount of prebreaking energy in frequency and direction band. Nonlinear transfers of energy to high frequencies that occur during breaking are not represented in the model.

Wind input. Waves grow through the transfer of momentum from the wind field to the wave field. The flux of energy, F_{in} , into the wave field in STWAVE is given by (Resio 1988a)

$$F_{in} = \lambda \frac{\rho_a}{\rho_w} 0.85 C_m \frac{u_*^2}{g} \quad (4)$$

where

λ = partitioning coefficient that represents the percentage of total atmosphere to water momentum transfer that goes directly into the wave field (0.75)

ρ_a = density of air, ρ_w is the density of water

C_m = mean wave celerity

u_* = friction velocity (equal to the product of the wind speed, U , and the square root of the drag coefficient, $C_D = .0012 + .000025U$)

In deep water, STWAVE provides a total energy growth rate that is consistent with Hasselmann et al. (1973).

The energy gain to the spectrum is calculated by multiplying the energy flux by the equivalent time for the wave to travel across a grid cell.

Because STWAVE is a half-plane model, only winds blowing toward the shore (+x direction) are included. Wave damping by offshore winds and growth of offshore-traveling waves are neglected.

Wave-wave interaction and white capping. As energy is fed into the waves from the wind, it is redistributed through nonlinear wave-wave interaction. Energy is transferred from the peak of the spectrum to lower frequencies (decreasing the peak frequency or increasing the peak period) and to high frequencies (where it is dissipated).

In STWAVE, the frequency of the spectral peak is allowed to increase with fetch (or equivalently propagation time across a fetch). The equation for this rate of change of f_p is given by

$$(f_p)_{i+1} = \left[(f_p)_i^{7/3} - \frac{9}{5} C \left(\frac{u_*}{g} \right)^{4/3} \Delta t \right]^{-3/7} \quad (5)$$

where the i and $i+1$ subscripts refer to the grid column indices within STWAVE and C is a dimensionless constant (Resio and Perrie 1989). The energy gained by the spectrum is distributed within frequencies on the forward face of the spectrum (frequencies lower than the peak frequency) in a manner that retains the self-similar shape of the spectrum.

Wave energy is dissipated (most notably in an actively growing wave field) through energy transferred to high frequencies and dissipated through wave breaking (white capping) and turbulent/viscous effects. There is a dynamic balance between energy entering the wave field because of wind input and energy leaving the wave field because of nonlinear fluxes to higher frequencies (Resio 1987, 1988a).

Numerical Discretization

STWAVE is a finite-difference numerical model, formulated on a Cartesian grid. Grid cells are square ($\Delta x = \Delta y$). Variable grid resolution can be obtained by nesting model runs. This is accomplished by running the model at a coarse resolution and saving a spectrum at a nearshore point. This nearshore spectrum can then be used as a boundary condition for another grid of finer resolution. STWAVE operates in a local coordinate system, with the x-axis oriented in the cross-shore direction (origin offshore) and the y-axis oriented alongshore, forming a right-handed coordinate system. The orientation of the x axis (± 87.5 deg) defines the half plane that is represented in the model. The y-axis is typically aligned with the bottom contours. Wave angles are defined in a mathematical sense, measured counterclockwise from the x-axis.

Lateral boundaries in the model can be specified as land or water by specifying the cell depths as positive (water) or negative (land). Note that specifying land around the entire grid will give different results than if the lateral boundaries are water. Land boundaries reduce wave growth near the boundary because they "block" propagation from landward directions. If the boundaries are specified as water, a zero-gradient type of boundary is applied that allows energy, consistent with neighboring cells, to propagate into or out of the domain along the lateral boundary.

Estimating nearshore wind-wave growth and transformation is a critical component of most coastal engineering projects, e.g., predicting bathymetric and shoreline change, estimating navigation channel shoaling and migration, designing or repairing coastal structures, assessing navigation conditions, and evaluating natural evolution of coastal inlets or beaches versus consequences of engineering actions. Nearshore wave propagation is influenced by complex bathymetry (including shoals and navigation channels); tide-, wind-, and wave-generated currents; tide- and surge-induced water-level variation; and coastal structures. Use of numerical wave models has become widespread to represent wave transformation primarily because of their increasing sophistication and economy of application relative to the large expense of field measurements or physical model studies.

STWAVE Application at Milwaukee Harbor

Input to STWAVE consists of bathymetric data, wave height, direction, period and wind speed. A bathymetric survey was performed in August 1999 by USACE, Kewaunee Area Office. This data was supplemented with National Ocean Survey (NOS) data. The bathymetry was input for approximately 60 miles, from Kenosha to Port Washington and is shown in Figure A-5. Winds were modeled from two general directions, from the northeast and southeast. The wind from the northeast represents the high-energy extra-tropical storm events that frequently occur during fall and spring. These waves must diffract through the breakwater openings or overtop the existing structure before reaching the beach and bluff. During these events littoral transport is generally from the north to the south. The wind from the southeast represents the lower-energy summer winds. This wave can enter behind the breakwater at the southern end. A rectilinear modeling grid was developed for both winds. The lakeward boundary of each grid passes through wave information study (WIS) station number 9.

Thirty-two years of hindcast data was examined in selecting the input waves for the two modeling grids. This wave data is summarized as a wave rose in Figure A-6.

The data file containing all 32 years of 3-hourly wave heights, direction and period is on the enclosed CD. Note that the greatest percentage of waves approach Milwaukee from the south, yet the largest waves are out of the north to northeast. Consequently, three angles of wave approach were selected for incorporation into the model. The 20° and 90° approach direction were selected to represent the large northeasterly storms and a 160° approach direction was selected to represent the prevailing southerly winds. Based on a statistical analysis of the 32-year hindcast of wave heights, a five-meter and a one-meter wave were selected as the input waves along the offshore boundary. The 5-meter wave represents a major storm event, having a recurrence interval of approximately 10 years. A wave spectrum was created based on a spectral peakedness parameter and directional spreading parameter of 3.3 and 4, respectively. One of the spectral wave energy distributions is shown in Figure A-7.

The STWAVE results for high-water scenario with winds out of the northeast are shown in Figure A-8. The STWAVE transformation produced a significant wave height (H_s) at the CGWAVE boundary of 4.0 m, given a 90° approach angle with a 5 m input wave. The significant wave height is the average wave height of the largest 1/3 of waves in the spectrum. By comparison, a simple TMA transformation produced an H_s of 4.36 m. The similarity of these results provides additional confidence in the model output.

STWAVE output was collected at an offshore point and was used as input to the wave agitation model, CGWAVE. The results of all STWAVE scenarios at this offshore monitoring station are summarized below:

Input Wave Direction	Input Wave Height (Period)	STWAVE Output at Monitoring Site			
		High Water Scenario		Low Water Scenario	
		H_s	Peak Period	H_s	Peak Period
20° (NNE)	5.0m (9.6sec)	4.18 m	9.1 sec	4.16 m	9.1 sec
20° (NNE)	1.0m (5.0sec)	0.95 m	4.8 sec	0.95 m	4.8 sec
90° (E)	5.0m (9.6sec)	3.98 m	9.1 sec	3.94 m	9.1 sec
90° (E)	1.0m (5.0sec)	0.95 m	4.8 sec	0.93 m	4.8 sec
160° (SSE)	5.0m (9.6sec)	3.76 m	9.1 sec	3.72 m	9.1 sec
160° (SSE)	1.0m (5.0sec)	0.82 m	4.8 sec	0.84 m	4.8 sec

Table A-1: Summary of STWAVE output at monitoring station

CGWAVE

Wave climate plays a very important role in all coastal projects. However, in most cases, little wave data are available for engineering construction and planning. Field

observation and physical modeling of waves are extremely difficult, costly, and time-consuming. Buoys are far away from the project site, and remote-sensing instruments do not systematically provide wave data at the desired resolution in the near shore region. Since no data-recording instrument can anticipate future "sea" states, the desired "sea"-state information may be obtained and plans evaluated with reliable mathematical modeling techniques. CGWAVE is a numerical model capable of predicting wave heights near complicated structures, such as Milwaukee's segmented offshore breakwater.

It is essential to have reliable information on wave conditions for many coastal engineering problems. The most important wave conditions for design and assessment in project studies in the area of interest include the wave heights, wave periods and the dominant wave propagation directions. Typically, these wave parameters are obtained from a wave transformation model that transfers the wave data collected at some remote deep-water site to the location of the project in the near shore. As waves move from deeper waters to approach the shore, these fundamental wave parameters will change as the wave speed changes and wave energy is redistributed along wave crests due to the depth variation between the transfer sites and the presence of islands, background currents, coastal defense structures, and irregularities of the enclosing shore boundaries and other geological features. Waves undergo the severest change inside the surf zone where wave breaking occurs and in the regions where reflected waves from coastline and structural boundaries interact with the incident waves.

Until recently, the linear wave ray theory was used for wave transformation by tracing rays from deep water to the project site near shore. The effects on wave propagation of the wave height and direction along the wave crest are ignored in the ray theory since this theory assumes that wave energy propagates only along a ray and thus, energy flux is conserved between two adjacent rays. As a consequence of this assumption, ray theory breaks down when wave ray crossings and caustics occur because the physics of diffraction are totally ignored in the numerical ray models.

Starting in the early 1980s, coastal designers and researchers have recognized the importance of the combined effects of refraction and diffraction and begun to develop improved theories and associated numerical models. There are indeed several wave theories available that could adequately describe the combined refraction and diffraction of waves from deep water to shallow water (Demirbilek and Webster 1992 and 1998). One of these is the mild-slope equation (MSE). This is a depth-averaged, elliptic type partial differential equation which ignores the evanescent modes (locally emanated waves) and assumes that the rate of change of depth and current within a wavelength is small, hence the 'mild-slope' acronym.

Numerous MSE-based numerical models have been developed for predicting the wave forces on offshore structure and studying wave fields around the offshore islands. Numerical, laboratory and field tests of the MSE models have shown that the MSE can provide accurate solutions to problems where the bottom slope is up to 1:3. From a practical standpoint, the computational requirements for solving the MSE are much

larger than those for ray tracing. The reasons for this are because the MSE is a two-dimensional equation and has to be solved as a boundary-value problem with appropriate boundary conditions. The entire domain of interest must be discretized and solved simultaneously and the element size has to be small enough that there are about 10 to 15 nodes within each wavelength. These requirements place severe demands on computer resources when applying MSE models to large coastal domains. The modeling domain at Milwaukee contains approximately 170,000 nodal points. One run on a personal computer requires approximately 70 hours to complete. There were 12 different water-level/wave height scenarios examined. After several initial runs on a PC, the remainder of the scenarios were run on a supercomputer at Engineering Research and Development Center (ERDC), Vicksburg, MS.

A difficult problem in prediction of waves in the near shore is to determine where approximately the wave breaking (and breaker line) occurs when waves are inside the surf zone. In numerical models presently used, location is not known a priori, and is usually selected with an ad hoc criteria based on the ration of wave height to local water depth. Bottom friction and dissipation from the surrounding land boundaries (i.e. entrance losses at the mouth of a harbor) may also be empirically incorporated into MSE models. A simplified version of the MSE is known as the 'parabolic approximation' (PA), which usually reduces the excessive computational demands of MSE model at the expense of further assumptions and simplifications which may render the numerical predictions inaccurate and inappropriate for many coastal and ocean engineering problems (Panchang et al. 1998).

The only purpose of adapting the PA is to convert the MSE to a set of simpler equations that describe a wave propagating in a prescribed direction while still taking both refraction and diffraction in the lateral direction into account. The greatest advantage of PA is its numerical efficiency, it can be solved rather easily by numerical means and thus could be used for predicting wave transformation over a relatively large coastal region. When reflection is of major interest, as it is in harbors, the MSE should be used since the PA ignores reflection. One must also be reminded that the PA that the length scale of the wave amplitude variation in the direction of wave propagation (x direction) is much longer than that in the transverse direction (y direction). The PA is derived on the assumption that percentage changes of depth within a typical wavelength are small compared to the wave slope. For details about PA models, see Booji (1981), Liu (1993), Kirby (1983), Liu and Tsay (1984), and Kirby and Dalrymple (1984). The PA has been verified extensively by laboratory studies and field application (Berkhoff et al. 1982), Liu and Tsay (1984), Kirby and Dalrymple (1984), Vincent and Briggs (1989), (Demirbilek 1994, Demirbilek et al. 1996a and 1996b), and Panching et al. (1998).

The mild-slope wave equation (also known as the "combined refraction-diffraction" equation), first suggested by Eckart (1952) and later re-derived by Berkhoff (1972, 1976) and others, is now well accepted as the method for estimating coastal wave conditions. It can be used to model a wide spectrum of waves, since it passes, in the limit, to the deep and shallow water equations. Although the equation was developed in

the mid-seventies, computational difficulties precluded the development of a model for the complete mild-slope equation (except for very small domains). Typically, coastal wave propagation problems involve the modeling of very large domains. For example, consider the case of 12-second waves of 15 m depth. The wavelength L is about 136 m; an 8 km domain is about $3600L^2$ in size. The difficulties associated with solving such large problems spawned the development of several simplified models (e.g. the "parabolic approximation" models (Dalrymple et al. 1984; Kirby, 1986, RCPWAVE model (Ebersole, 1985), EVP model (Panchang et al 1988), etc.). However, these simplified models compromised the physics of the mild-slope equation: they model only one- or two-way propagation with weak lateral scattering. Such models are hence applicable only to rectangular water domains for a very limited range of wave directions and frequencies. Most realistic coastal domains with arbitrary wave scattering cannot be modeled with these simplified models.

CGWAVE was developed at the University of Maine under a contract for the U.S. Army Corps of Engineers, Waterways Experiment Station (Demirbilek, 1998). CGWAVE is a general purpose, state-of-the-art wave prediction model. It is applicable to estimation of wave fields in harbors, open coastal regions, coastal inlets, around islands, and around fixed or floating structure. While CGWAVE simulates the combined effects of wave refraction-diffraction included in the basic mild-slope equation, it also includes the effects of wave dissipation by friction, breaking, nonlinear amplitude dispersion, and harbor entrance losses. CGWAVE is a finite-element model that is interfaced to the SMS model (Jones & Richards, 1992) for graphics and efficient implementation (pre-processing and post-processing). The classical super-element method as well as a new parabolic approximation method developed recently (Xu, Panchang and Demirbilek 1996), are used to treat the open boundary condition. An iterative suggested procedure (conjugated gradient method) introduced by Panchang et al (1991) and modification suggested by Li (1994) are used to solve the discretized equations, this enabling the modeler to deal with large domain problems.

BASIC EQUATIONS (CGWAVE)

The solution of the two-dimensional elliptic mild-slope wave equation is a well-accepted method for modeling surface gravity waves in coastal areas (e.g. Chen & Houston, 1987; Chen, 1990; Xu & Panchang, 1993; Mei, 1983; Berkhoff, 1976; Kostense et al. 1986; Tsay and Liu, 1983). This equation may be written as:

$$\nabla \cdot (CC_g \nabla \hat{\eta}) + \frac{C_g}{C} \sigma^2 \hat{\eta} = 0 \quad (6)$$

Where

$\hat{\eta}(x, y)$ = complete surface elevation function, from which the wave height can be estimated

σ = wave frequency under consideration (in radian/second)

$C(x, y)$ = phase velocity = σ/k

$C_g(x, y)$ = group velocity = $\partial\sigma/\partial k = nC$ with

$$n = \frac{1}{2} \left(1 + \frac{2kd}{\sinh 2kd} \right) \quad (7)$$

$k(x, y)$ = wave number ($=2\pi/L$), related to the local depth $d(x, y)$ through the linear dispersion relation:

$$\sigma^2 = gk \tanh(kd) \quad (8)$$

Equation 7 simulated wave refraction, diffraction, and reflection (i.e. the general wave scattering problem) in coastal domains of arbitrary shape. However, various other mechanisms also influence the behavior of waves in a coastal area. The mild-slope equation can be modified as follows to include the effects of frictional dissipation (Dalrymple et al. 1984; Liu and Tsay 1985) and wave breaking (Dally et al. 1985; De Girolamo et al. 1988):

$$\nabla \cdot (CC_g \nabla \hat{\eta}) + \left(\frac{C_g}{C} \sigma^2 + i\sigma w + iC_g \sigma \gamma \right) \hat{\eta} = 0 \quad (9)$$

where w is a friction factor and γ is a wave breaking parameter. Following Dalrymple et al. (1984), we have used the following form of the damping factor in CGWAVE:

$$w = \left(\frac{2n\sigma}{k} \right) \left[\frac{2f_r}{3\pi} \frac{ak^2}{(2kd + \sinh 2kd) \sinh kd} \right] \quad (10)$$

where a ($= H/2$) is the wave amplitude and f_r is a friction coefficient to be provided by the user. The coefficient f_r depends on the Reynolds number and the bottom roughness and may be obtained from Madsen (1976) and Dalrymple et al. (1984). Typically, values for f_r are in the same range as for Manning's dissipation coefficient 'n'. Specifying f_r as a function of (x, y) allows the modeler to assign larger values for elements near harbor entrances to simulate entrance loss. For the wave breaking parameter γ , we use the following formulation (Dally et al. 1985, Demirbilek 1994, Demirbilek et al. 1996b):

$$\gamma = \frac{\chi}{d} \left(1 - \frac{\Gamma^2 d^2}{4a^2} \right) \quad (11)$$

where χ is a constant (a value of 0.15 is used in CGWAVE following Dally et al (1985)) and Γ is an empirical constant (a value of 0.4 is used in CGWAVE).

In addition to the above mechanisms, nonlinear waves may be simulated in the MSE. This is accomplished by incorporating amplitude-dependent wave dispersion, which has been shown to be important in certain situations (Kirby and Dalrymple 1986). The nonlinear dispersion relation used in place of Equation 8 is

$$\sigma^2 = gk \left[1 + (ka)^2 F_1 \tanh^5 kd \right] \tanh \{ kd + kaF_2 \} \quad (12)$$

where

$$\left. \begin{aligned} F_1 &= \frac{\cosh(4kd) - 2\tanh^2(kd)}{8\sinh^4(kd)} \\ F_2 &= \left(\frac{kd}{\sinh(kd)} \right)^4 \end{aligned} \right\} \quad (13)$$

Harbor Application

The finite-element formulation given above is for open-sea offshore problems. In case of harbor problems, the formulation is analogous. The only difference arises from the treatment of the open boundary condition. The classical treatment of these problems assumes that the coastlines outside the model domain are straight, collinear, and fully reflective. The exterior wave field written as $\hat{\eta}_{\text{ext}} = \hat{\eta}_I + \hat{\eta}_R + \hat{\eta}_S$, where $\hat{\eta}_I$, $\hat{\eta}_R$, and $\hat{\eta}_S$ represent the incident, the reflected, and the scattered wave fields, respectively. Based on the assumptions, we define (Demirbilek and Gaston 1985)

$$\begin{aligned} \hat{\eta}_0 &= \hat{\eta}_I + \hat{\eta}_R \\ &= Ae^{ikr\cos(\theta-\theta_1)} + Ae^{ikr\cos(\theta+\theta_1)} \\ &= 2A \sum_{n=0}^{\infty} \varepsilon_n i^n J_n(kr) \cos n\theta_1 \cos n\theta \end{aligned} \quad (14)$$

where A is the incident wave amplitude and θ_1 is the incident wave angle with respect to the exterior coastlines. The scattered wave potential $\hat{\eta}_S$ in the exterior region must take the following form in order to comply with the exterior coastline boundary conditions:

$$\hat{\eta}_S = \sum_{n=0}^{\infty} H_n(kr) \alpha_n \cos n\theta \quad (15)$$

as shown in Xu, Panshang and Demirbilek (1995). The finite-element formulation of harbor problems can now readily be found in a manner similar to the open-sea

problems described above, by replacing $\hat{\eta}_l$ and $\hat{\eta}_s$ and performing the boundary integration for l_4 through l_6 from 0 to π .

GENERATION OF FINITE-ELEMENT NETWORK

CGWAVE requires a two-dimensional (2D) triangle grid network for its finite-element calculations. Although several grid generation packages are available, they are not suitable for elliptic coastal wave models for which the size of the elements must be related to the wave length (which varies with local water depth) for proper resolution. A semicircular open boundary has to be created for special open boundary treatment, and reflection coefficients, which may vary from one part of the coastal boundary to another, are also required as input data for the model. To deal with these special problems, CGWAVE has been interfaced with the grid-generator associated with the SMS (Surface water Modeling Systems) flow modeling package. The Engineering Computer Graphics Laboratory is developing this state-of-the-art package for the US Army Corps of Engineers at Brigham Young University.

SMS contains a set of 2D hydrodynamic models and a general-purpose grid generation and visualization package. SMS includes an efficient finite-element grid-generator. However, this grid-generator was originally designed for other types of hydrodynamic models. Three utility programs that help interface CGWAVE with the SMS grid-generator have been developed for use outside SMS, prior to the full integration of CGWAVE into SMS. Given a coarse rectangular array of bathymetric data, these programs generate a wavelength-dependent triangular nodal network (based on the user-specific resolution, i.e. the number of points per wave length), automatically construct the semi-circular open boundary, assign reflection coefficients along the coastal boundaries, eliminate unwanted land points, etc. The resulting grid and boundary data from SMS are then filtered by another utility program for use by the wave model. The output from the wave model can be processed and then plotted by using SMS. This makes model implementation very efficient and allows the user to view a graphic representation of the solution.

CGWAVE at Milwaukee Harbor and Results

A finite-element mesh was constructed in SMS containing approximately 170,000 nodal points. The boundary of the modeling domain is shown in Figure A-9. Descriptions of the 12 CGWAVE scenarios are summarized in Table A-2.

High/Low Water Effects

Four alternatives were modeled under a low-water scenario. These are shown in Table A-2 as cases 1-4 and contain simulations of waves from all three approach angles. Figures A-10 and A-11 show a comparison of the wave climate for a high water and low water scenario. The still-water elevation for the low water scenario was set to

577.5 ft, IGLD 1985 or at low-water datum (LWD). The wave energy striking the shore along Bayview Park is similar for these two scenarios. Note however, that during low-water events, significantly more wave energy is concentrated near the southern opening of the breakwater. It appears that during low water these waves are refracted and focused on this section of coast. During the site visit, it was observed that this section of coast is heavily protected with armor stone, likely the results of energetic wave activity, such as that predicted by the model. The remaining 8 runs were performed at a relatively high still-water level, 582.7 ft, IGLD 1985 or +5.2 LWD. The high still-water level approximately corresponds to a 20-yr recurrence interval. It was observed that along Bayview Park there was little difference in wave climate between the high and low water scenarios.

Case number	Geometry modeled	Water-level modeled	Input wave direction	Input wave amplitude	Input wave period
Case 1	Current configuration	Low-water scenario	20°	2.08 m	9.1 sec
Case 2	Current configuration	Low-water scenario	90°	2.0 m	9.1 sec
Case 3	Current configuration	Low-water scenario	160°	0.42 m	4.8 sec
Case 4	Current configuration	Low-water scenario	160°	1.86 m	9.1 sec
Case 5	Current configuration	High-water scenario	20°	2.09 m	9.1 sec
Case 6	Current configuration	High-water scenario	90°	2.0 m	9.1 sec
Case 7	Current configuration	High-water scenario	160°	1.88 m	9.1 sec
Case 8	Current configuration	High-water scenario	160°	0.42 m	4.8 sec
Case 9	No openings	High-water scenario	20°	2.09 m	9.1 sec
Case 10	No openings	High-water scenario	160°	1.88 m	9.1 sec
Case 11	Breakwater removed	High-water scenario	20°	2.09 m	9.1 sec
Case 12	Breakwater removed	High-water scenario	160°	1.88 m	9.1 sec

Table A-2: Summary of CGWAVE input parameters

Model Results

To assess the effects of modifications to the breakwater, three different geometric configurations of the breakwater were modeled. The first scenario represents the current breakwater in its present condition. This configuration and the nearshore bathymetry are shown in Figure A-12. The modeling results for these scenarios (Cases 1-8) are shown in Figures A-13 through A-20.

The second geometric configuration represents a continuous breakwater (no segmented openings) and is shown in Figure A-21. The modeling results for these scenarios (Cases 9 and 10) are shown in Figures A-22 and A-23.

The final orientation examined the removal of the county breakwater (Figure A-24). The results of these scenarios (Cases 11 and 12) are shown in Figures A-25 and A-26. The output for all the modeled scenarios is enclosed on a CD if further examination is desired.

An example of the finite element grid near the north opening is shown in Figure A-27.

Conclusions

The wave climates, as displayed in Figures A-13 through A-26, show varying quantities of wave energy in the lee of the breakwater and along the beach. In its present state, the breakwater provides significant protection to the beach and bluff. Figures A-22 and A-23 suggest closing the gaps in the breakwater would provide minimal additional protection to the beach and bluff. Closing the gaps is also likely to cause stagnation of the water behind the breakwater, possibly resulting in water quality and aesthetic problems. Moreover, vessels would be required to travel a greater distance before reaching the sheltered water behind the structure. It is also likely that a channel would have to be designated and maintained in these shallow waters if this option were implemented.

Removal of the segmented offshore breakwater will allow significant wave energy to reach the beach and bluff (Figure A-25). The construction of a stone revetment along this bluff, in conjunction with removal of the breakwater, would provide protection from attacking waves at the expense of the beach. The beach would begin to erode. Furthermore, it is very likely that the resulting beach along Bayview Park would be very narrow or possibly disappear. It is beyond the scope of this study to quantify the time required for the beach to erode; however, it is expected to be a considerable amount of time, as there is a large quantity of sand impounded between the breakwater and the bluff. It has been estimated that approximately 3 million yd³ of sand would be eroded from the beach and nearshore if the breakwater were removed. Furthermore, the construction of a stone revetment would limit access to the shore.

Based on the modeling results presented in this report, it is recommended that the existing breakwater remain offshore as a segmented breakwater. This configuration provides the best combination of shore protection, adequate water circulation and harborage for vessels during storms. The current navigation hazard posed by the submerged nature of several sections of the breakwater can be mitigated by placing buoys to note the presence of a submerged section. Furthermore, a notice to mariners should be issued describing the hazard and the proposed mitigation.

The final alternative is the rehabilitation of the existing breakwater. In its current condition, the breakwater has differentially consolidated, resulting in sections that are lower than others. In some instances, the low sections are under water. Furthermore,

some armor units have been displaced due to breaking waves and ice rafting. Concern has been raised that gaps resulting from subsidence of the structure may allow a large quantity of wave energy to pass the structure and reach the beach and bluff. It is the conclusion of this study that most wave energy will be excluded from the lee of the structure even with the breakwater in its dilapidated condition. The breakwater in its present condition is adequate to prevent most wave energy from passing the breakwater. The structure will cause storm waves to break as they pass over the structure, resulting in the loss of most wave energy to turbulent mixing.

References

- Battjes, J.A. (1982). "A case study of wave height variations due to currents in a tidal entrance." *Coast. Engrg.*, 6, 47-57.
- Battjes, J.A., and Janssen, J.P.F.M. (1978). "Energy loss and set-up due to breaking of random waves." *Proc. 16th Coast. Engrg. Conf.*, ASCE, 569-587.
- Berkhoff, J.C.W., Booij, N., and Radder, R.C. (1982). "Verification of numerical wave propagation models for simple harmonic linear waves." *Coast. Engrg.*, 6, 255-279
- Berkhoff, J.C.W. (1976). "Mathematical models for simple harmonic linear water waves wave refraction and diffraction." *Publ. 163*, Delft Hydraulics Laboratory.
- Berkhoff, J.C.W. (1972). "Computation of combined refraction-diffraction." *Proc. 13th Intl. Coast. Engrg. Conf.*, 741-790.
- Chen, H.S. (1990) "Infinite Elements for water wave radiation and scattering." *Intl. J. Num. Meth. In Fluids*, 11,555-569.
- Chen, H.S., and Houston, J.R. (1987). "Calculation of Water Level Oscillations in Harbors." *Instructional Report CERC-87-2*, Waterways Experiment Station, Vicksburg, Miss.
- Dally, W.R., Dean, R.G., and Dalrymple, R.A. (1985) "Wave height variation across beaches of arbitrary profile." *J. Geophys. Res.*, 90, 1917-11927.
- Dalrymple, R.A., Kirby, J.T., and Hwang, P.A. (1984). "Wave refraction due to areas of high energy dissipation." *J. Wtrway, Port, Coast., and Oc. Engrg.*, 110, 67-79.
- Davis, J.E. (1992). "STWAVE theory and program documentation." Chapter 8 in Coastal Modeling System User's Manual, *Instructional Report CERC-91-1*, Supplement 1, Ed. M.A. Cialone, Waterways Experiment Station, Vicksburg, Miss.
- Demirbilek, Z. (1994). "Comparison between REFDIFS and CERC Shoal Laboratory Study." *Unpubliashed Report*, Waterways Experiment Station, Vicksburg, Miss.
- Demirbilek, Z., and Gaston, J.D. (1985). "Nonlinear wave loads on a vertical cylinder." *Oc.Engrg.*, 12, 375-385.
- Demirbilek, Z. and Webster, W.C. (1992). "Application of the Green-Naghdi Theory of fluid sheets to shallow-water wave problems, Report 1: Model development, Report 2:User's manual and examples for GNWAVE" *Tech. Reports CERC-92-1 and CERC-92-13*, Waterways Experiment Station, Vicksburg, Miss.
- Demirbilek, Z., XU, B., and Panchang, V. (1996a). "Uncertainties in the validation of harbor wave models." *Proc. 25th Intl. Coast. Engrg. Conf.*, 1256-1267.
- Demirbilek, Z., Briggs, M., and Green, D. (1996b). "Wave-current interaction at Inlets." *Proc. 25th Intl. Coast. Engrg. Conf.*, 1219-1232.
- De Girolamo, P., Kostense, J.K., and Dingemans, M.W. (1988). "Inclusion of wave breaking in a mild-slope model." Computer Modeling in Ocean Engineering, Balkema, Rotterdam, 221- 229.

- Ebersole, B.A. (1985). "Refraction-diffraction model for linear water waves." *J. Wtrway., Port, Coast., and Oc. Engrg.*, 111,6.
- Hasselmann, K., Barnett, T.P., Bouws, E., Carlson, H., Cartwright, D.E., Enke, K., Ewing, J.A., Gienapp, H., Hasselmann, D.E., Kruseman, P., Meerburg, A., Muller, P., Olbers, D.J., Richter, K., Sell, W., and Walden, H. (1973). "Measurements of wind-wave growth and swell decay during the Joint North Sea Wave Project (JONSWAP)," *Deut. Hydrogr. Z., Suppl. A*, 8(12), 1-95.
- Jones, N.L., and Richards, D.R. (1992). "Mesh generation for estuarine flow models." *J. Wtrway., Port, Coast., and Oc. Engrg.*, 118, 599-614.
- Jonsson, I.G. (1990). "Wave-current interactions." Chapter 3 in *The Sea*, Vol.9, Part A, John Wiley & Sons, Inc., New York.
- Kirby, J.T. (1986). "Higher order approximation in the parabolic equation method for water waves." *J. Geophys. Research*, 91, 933-952.
- Kirby, J.T., and Dalrymple, R.A. (1984) "Verification of a parabolic equation for propagation of weakly-nonlinear waves." *Coast. Engrg.*, 8, 219-232.
- Kirby, J.T. and Dalrymple, R.A. (1986). "An approximate model for nonlinear dispersion in monochromatic wave propagation models." *Coast. Engrg.*, 9, 545-561.
- Kostense, J.K., Meijer, K.L., Dingemans, M.W., Mynett, A.E., and van den Bosch, P. (1986). "Wave energy dissipation in arbitrarily shaped harbours of variable depth." *Proc. 20th Intl. Conf. Coast. Engrg.*, 2002-2016
- Li, B. (1994). "A generalized conjugate gradient model for the mild slope equation." *Coast. Engrg.*, 23, 215-225.
- Liu, P.F.-F., and Tsay, T.K. (1984). "Refraction-diffraction model for weakly nonlinear water waves." *J. Fluid Mech.*, 141, 265-274.
- Madsen, O.S. (1976). "Wave climate of the continental margin: Elements of its mathematical description." Marine Sediment Transport and Environmental Management, John Wiley, New York.
- Mei, C.C. (1983). The Applied Dynamics of Ocean Surface Waves. John Wiley, New York.
- Miche, M. (1951). "Le Pouvoir reflechissant des ouvrages maritimes exposes a l' action de la houle." *Annals des Ponts et Chaussess*, 121e Annee, 285-319 (translated by Lincoln and Chevron, Univ. Calif., Berkley, Wave Research Laboratory, Series 3, Issue 363, June 1954).
- Panchang, V.G., Cushman-Roisin, B., and Pearce, B.R. (1988). "Combined refraction-diffraction of short waves for large coastal regions." *Coastal Engrg.*, 12, 133-156.
- Panchang, V.G., Ge, W., Cushman-Roisin, B., and Pearce, B.R. (1991). "Solution to the mild-slope wave problem by iteration." *Applied Ocean Research*, 13, 187-199.
- Resio, D.T. (1987). "Shallow-water waves. I: theory." *J. Wtrway., Port, Coast., and Oc. Engrg.*, ASCE, 264-281.
- Resio, D.T. (1988a). "Shallow-water waves. II: data comparisons." *J. Wtrway., Port, Coast., and Oc. Engrg.*, ASCE, 114(1), 50-65.

- Resio, D.T. (1988b). "A steady-state wave model for coastal applications." *Proc. 21st Coast. Engrg. Conf.*, ASCE, 929-940.
- Resio, D.T., and Perrie, W. (1989). "Implications of an f^4 equilibrium range for wind-generated waves." *J. Phys. Oceanography*, 19, 193-204.
- SWRPC, T.B. Evil, D.M. Michel son and J.A. Chapman. (1997). "Lake Michigan Shoreline recession and bluff stability in southeastern Wisconsin: 1995." Technical Report Number 36.
- Smith, J.M., Resio, D.T., and Vincent, C.L. (1997). "Current-induced breaking at an idealized inlet." *Proc. Coastal Dynamics '97*, ASCE, 993-1002.
- Smith, S.J., and Smith J.M. (1998). "Modeling waves at Ponce de Leon Inlet, Florida." Submitted to *J. Wtrway., Port, Coast., and Oc. Engrg.*, ASCE.
- Tsay, T.-K., and Liu, P.L.-F. (1983). "A finite element model for wave refraction and diffraction." *App. Oc. Res.*, 5, 30-37.
- Vincent, C.L., and Briggs, M.J. (1989). "Refraction-diffraction of irregular waves over a mound." *J. Wtrway., Port, Coast and Oc. Engrg.*, 115, 269-284.
- Xu, B., and Pachang, V.G. (1993) "Outgoing boundary conditions for elliptic water wave models." *Proc., The Royal Soc. Of Lon., Series A*, 441, 575-588.
- Xu, B., Panchang, V.G., and Demirebilek, Z. (1996) "Exterior reflections in elliptic harbor wave models

FIGURES

COASTAL HYDRODYNAMIC ANALYSIS

**U.S. Army Corps of Engineers
Detroit District
Great Lakes Hydraulics and Hydrology Office**

December 2000

Milwaukee, Wisconsin

Lake Michigan

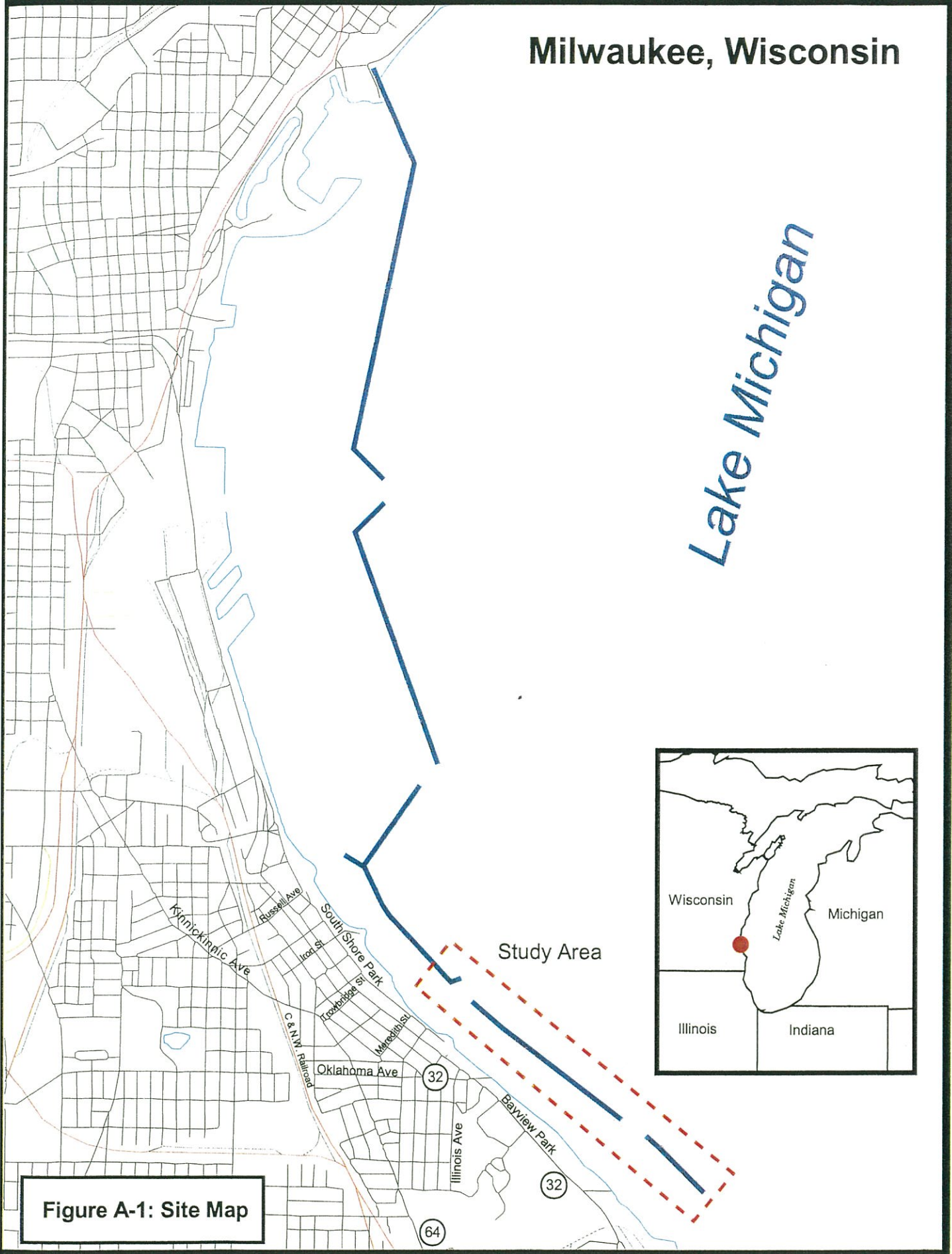


Figure A-1: Site Map



Figure A-2: Extent of SHOALS coverage during 1998 survey. Green zone represents acceptable SHOALS data.

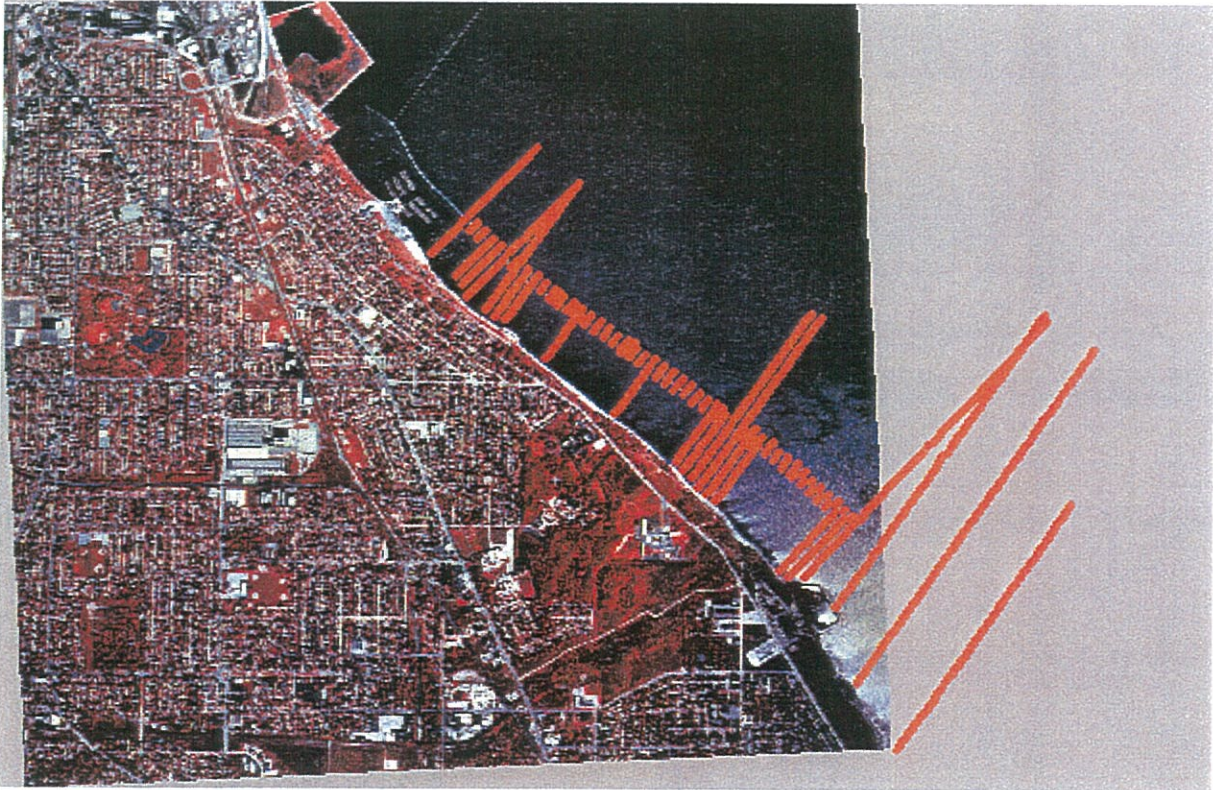


Figure A-3: Spatial extent of conventional hydrographic survey

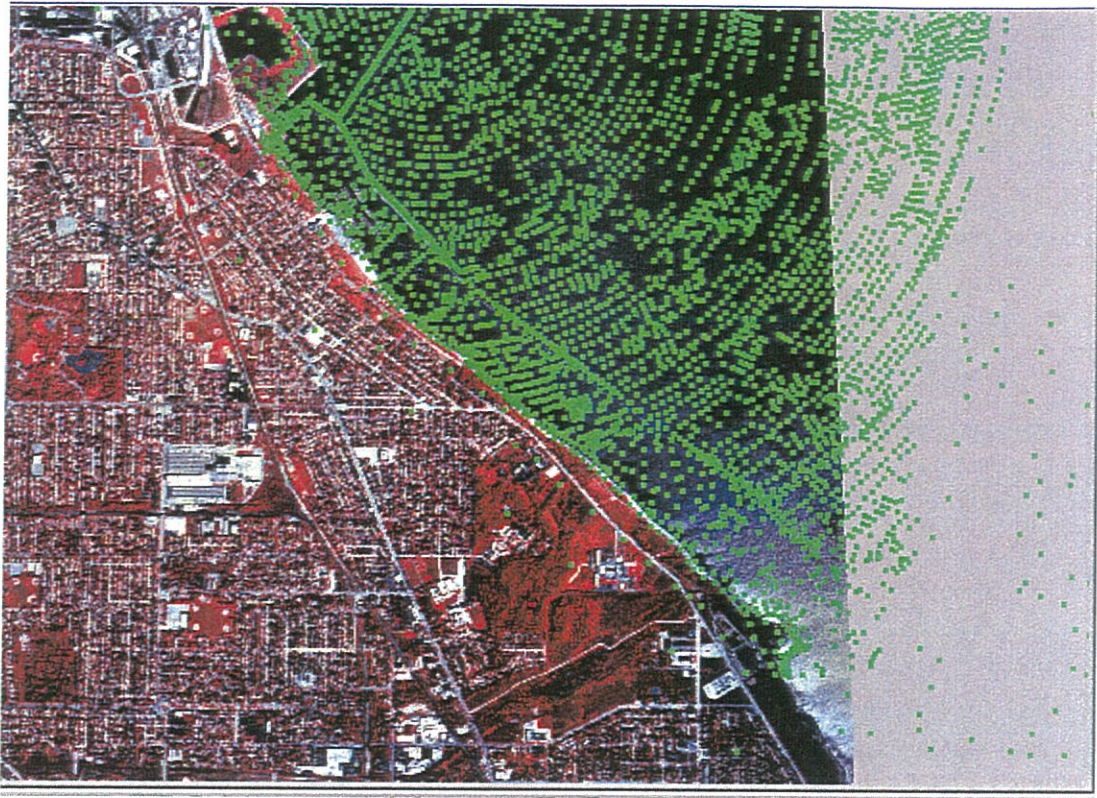


Figure A-4: Spatial extent of NOS survey

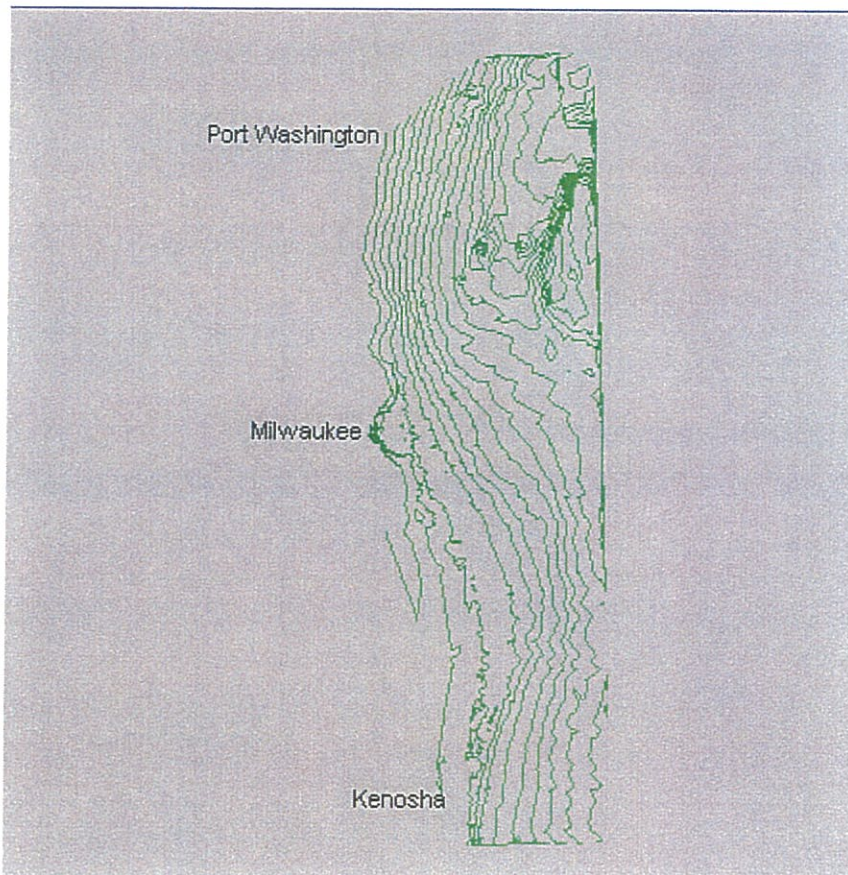


Figure A-5: Limits of STWAVE bathymetric domain

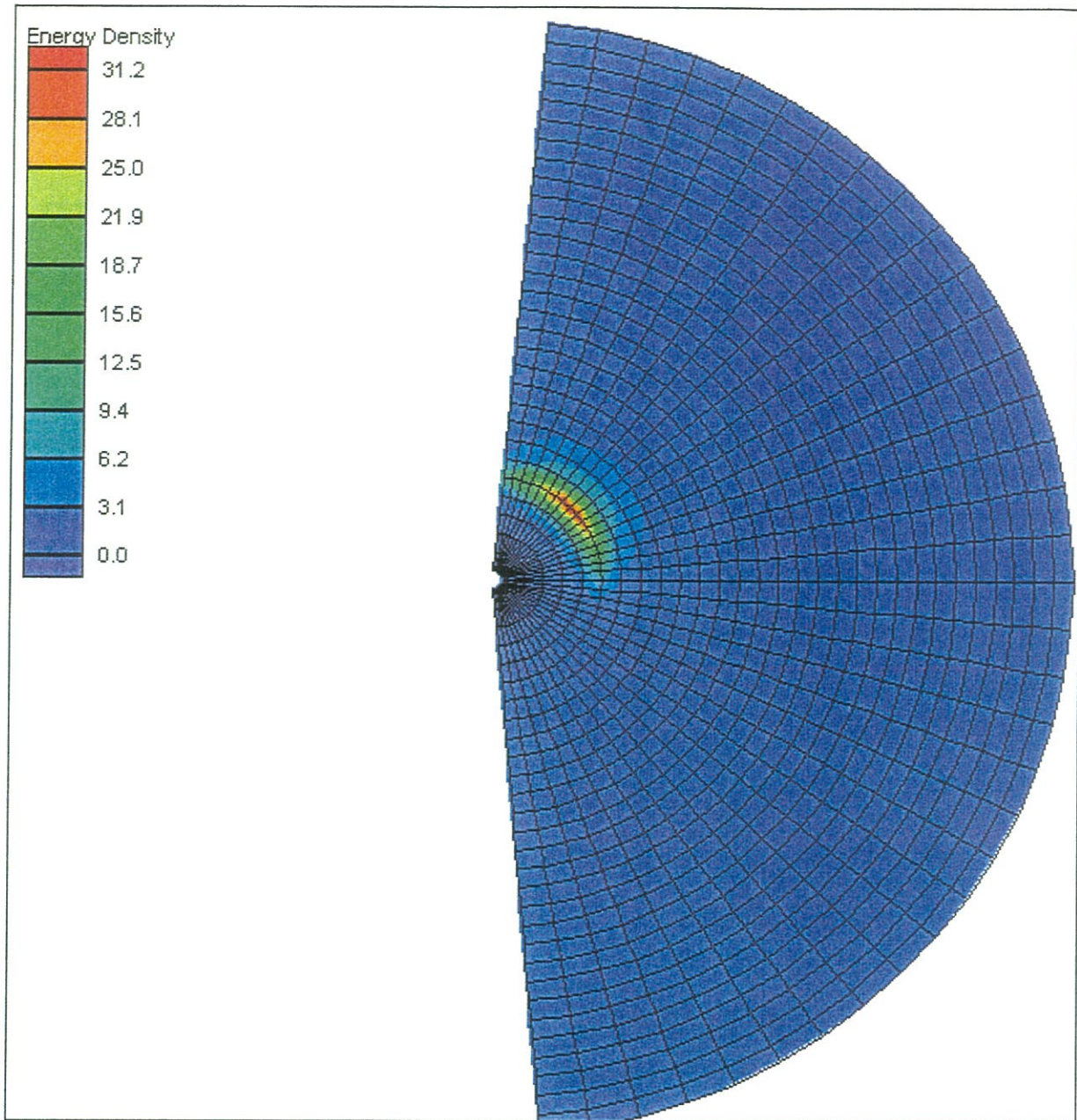


Figure A-6: WIS hindcast wave rose (1956-1987)

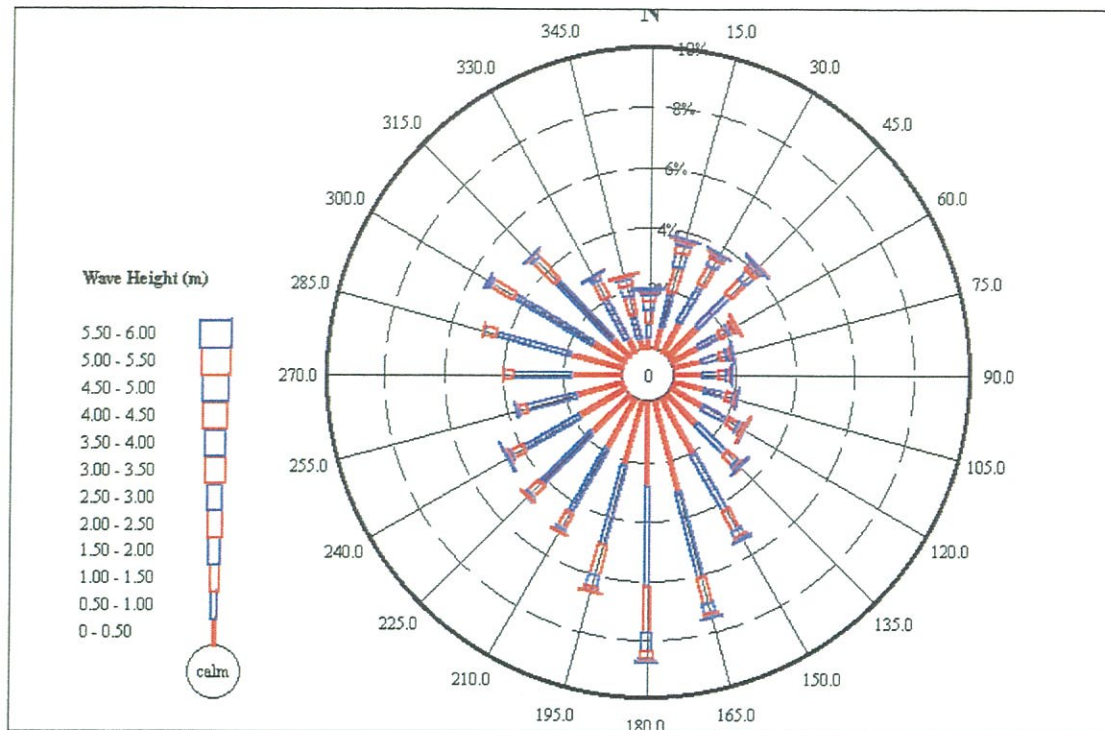


Figure A-7: Spectral energy distribution for northeasterly storm event

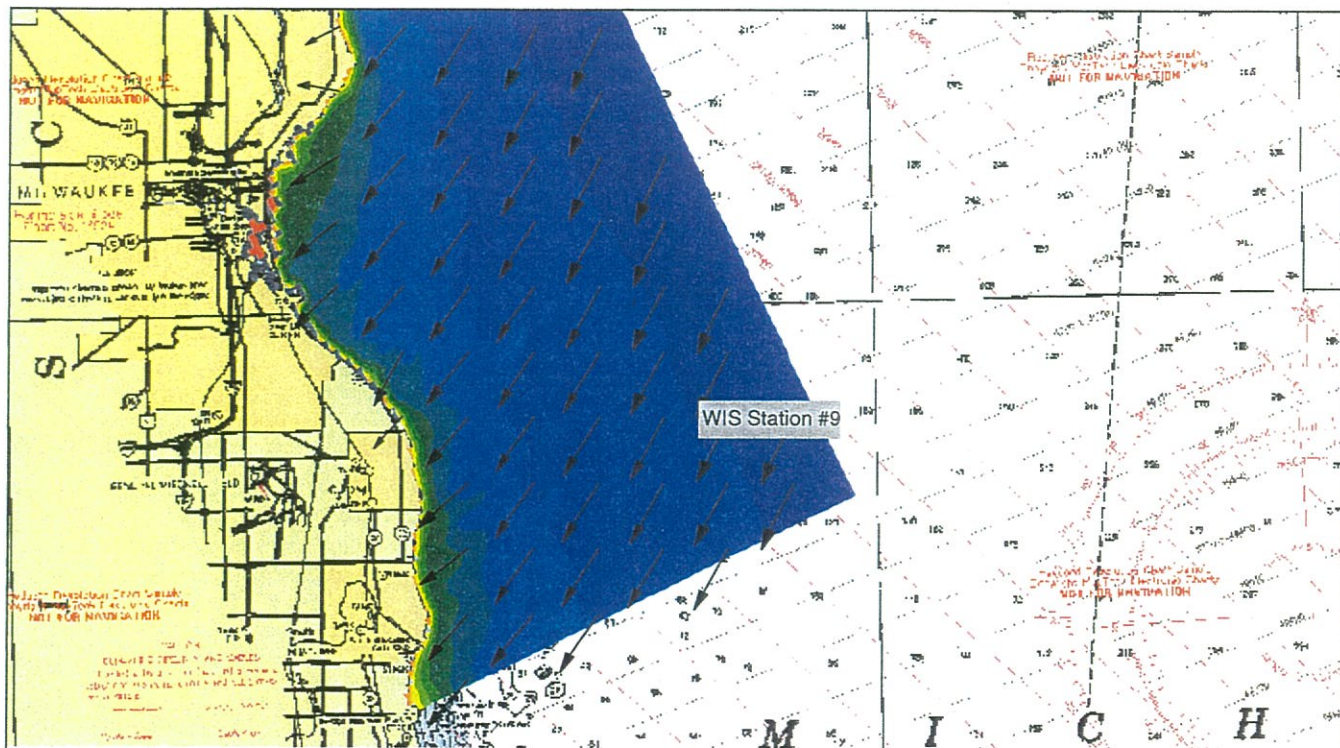


Figure A-8: STWAVE results for northeasterly storm

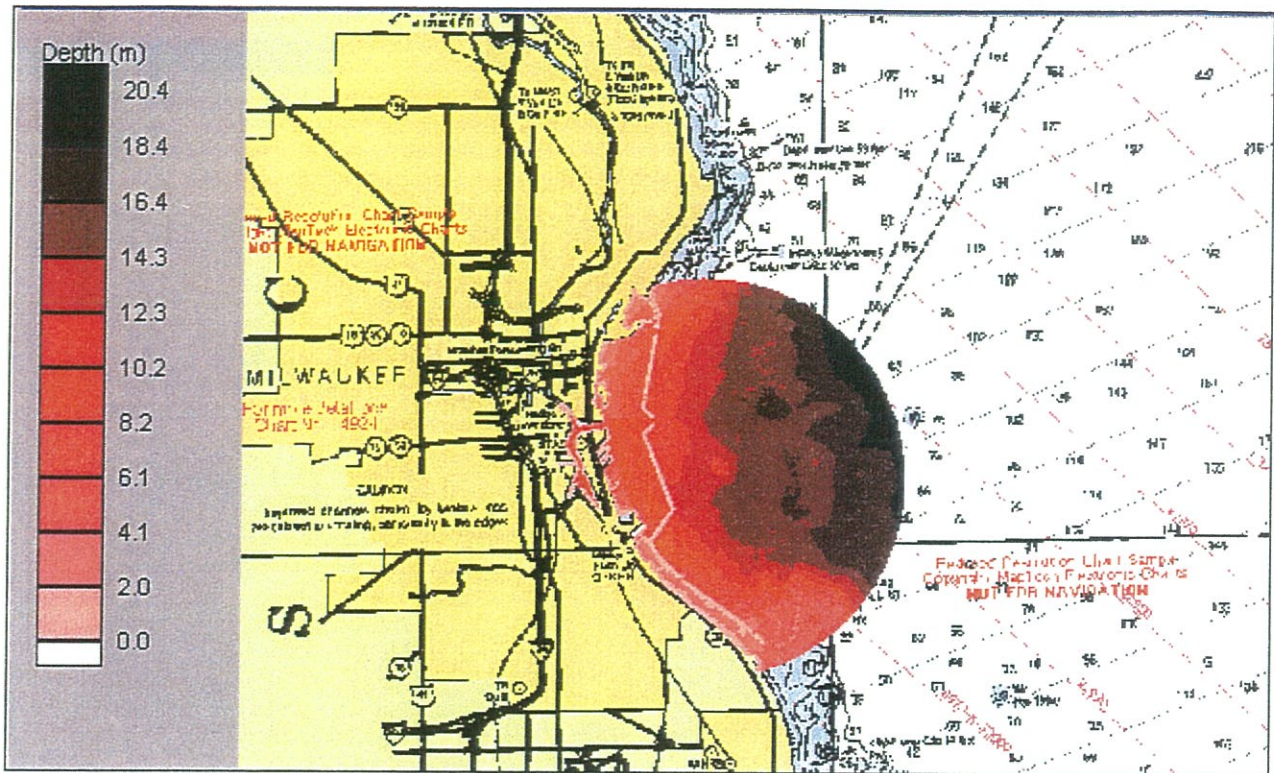


Figure A-9: CGWAVE modeling domain with color-coded bathymetry

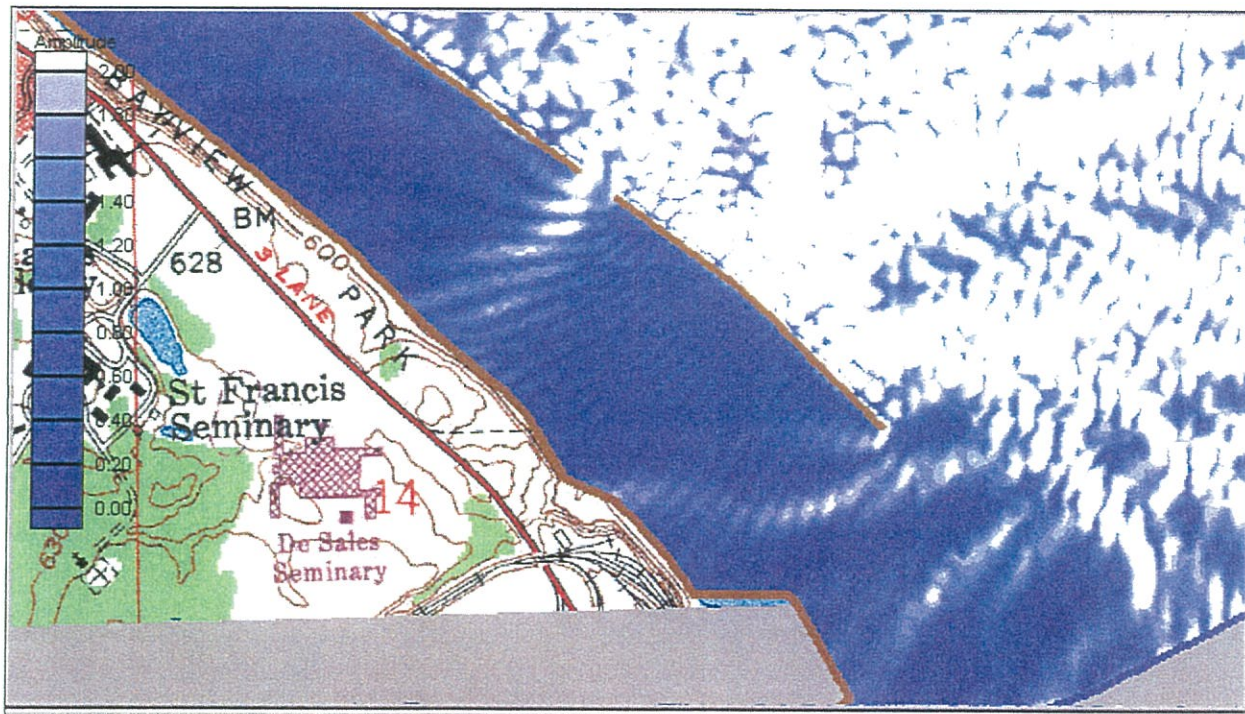


Figure A-10: High-water wave climate

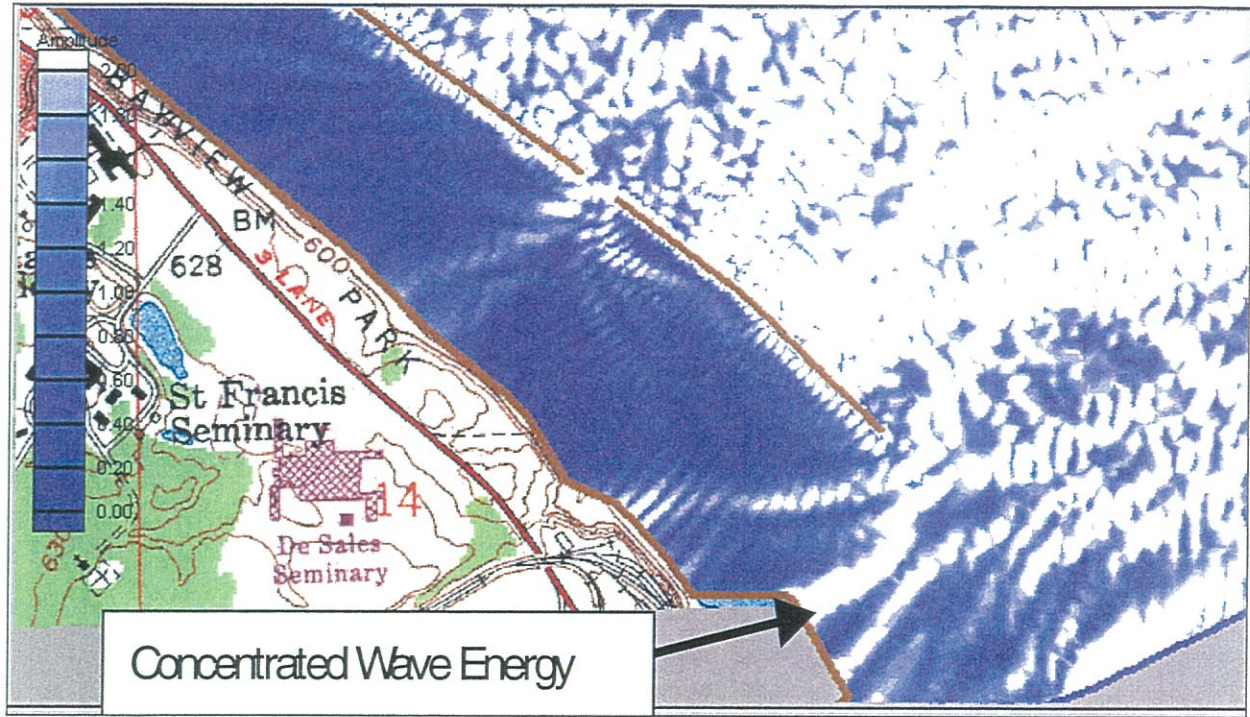


Figure A-11: Low-water Wave Climate

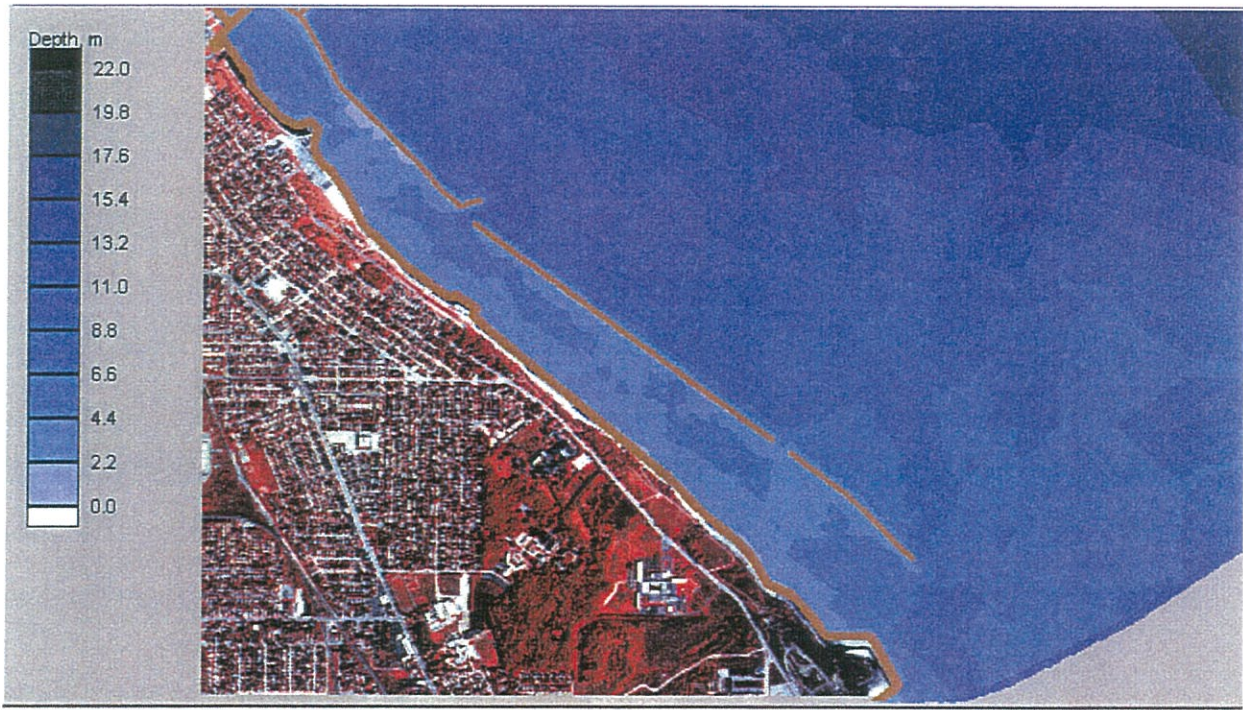


Figure A-12: Existing breakwater configuration and bathymetry

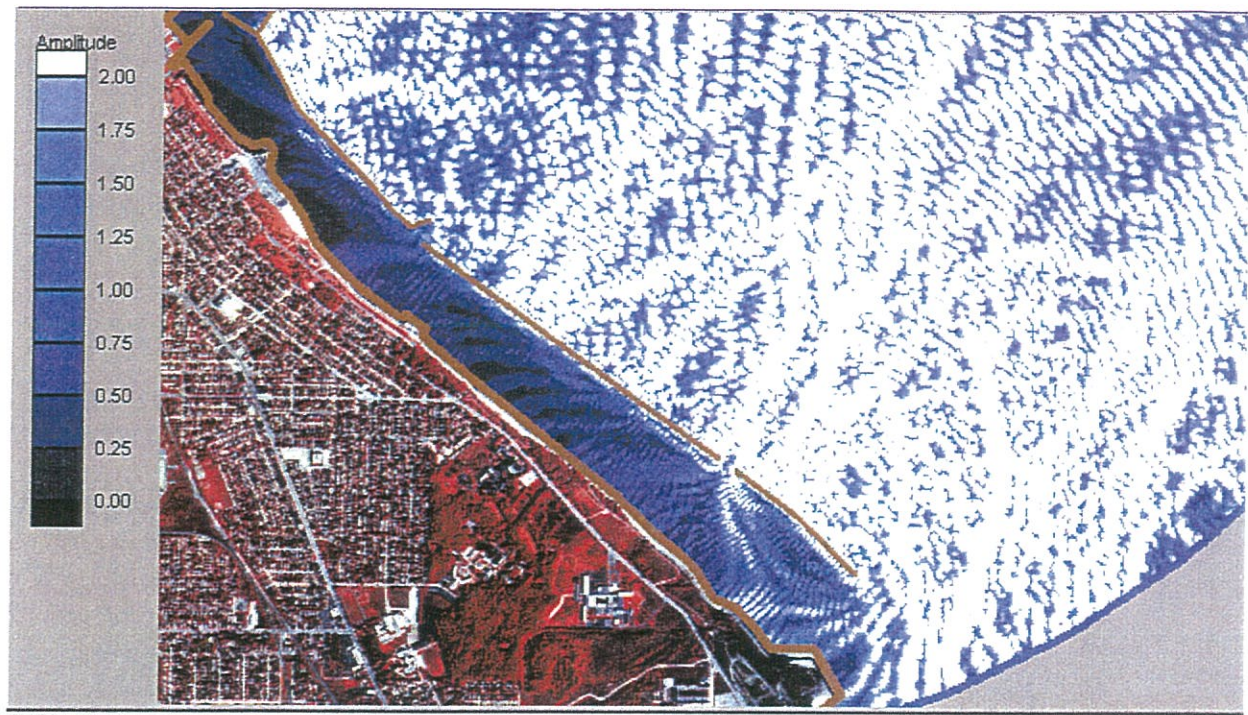


Figure A-13: Case 1 model output with 20 degree wave approach, 5m input wave-height and low SWE

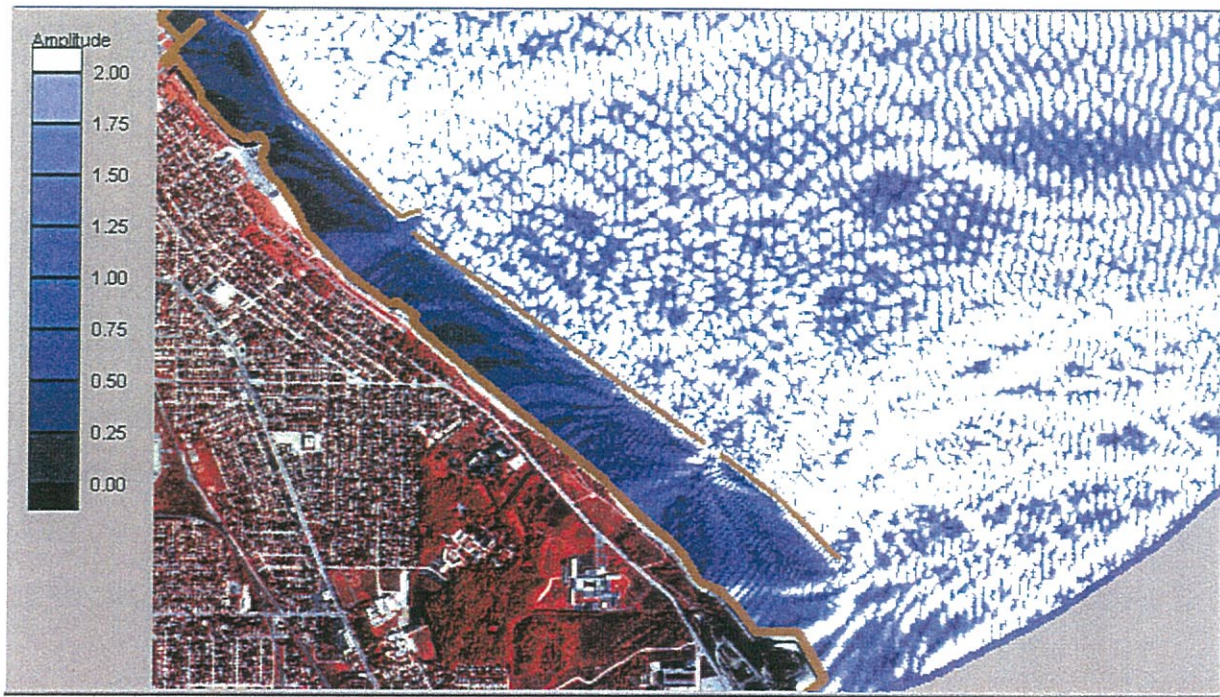


Figure A-14: Case 2 model output with 90 degree wave approach, 5m input wave-height and low SWE



Figure A-15: Case 3 model output with 160 degree wave approach, 1m input wave-height and low SWE



Figure A-16: Case 4 model output with 160 degree wave approach, 5m input wave-height and low SWE



Figure A-17: Case 5 model output with 20 degree wave approach, 5m input wave-height and high SWE

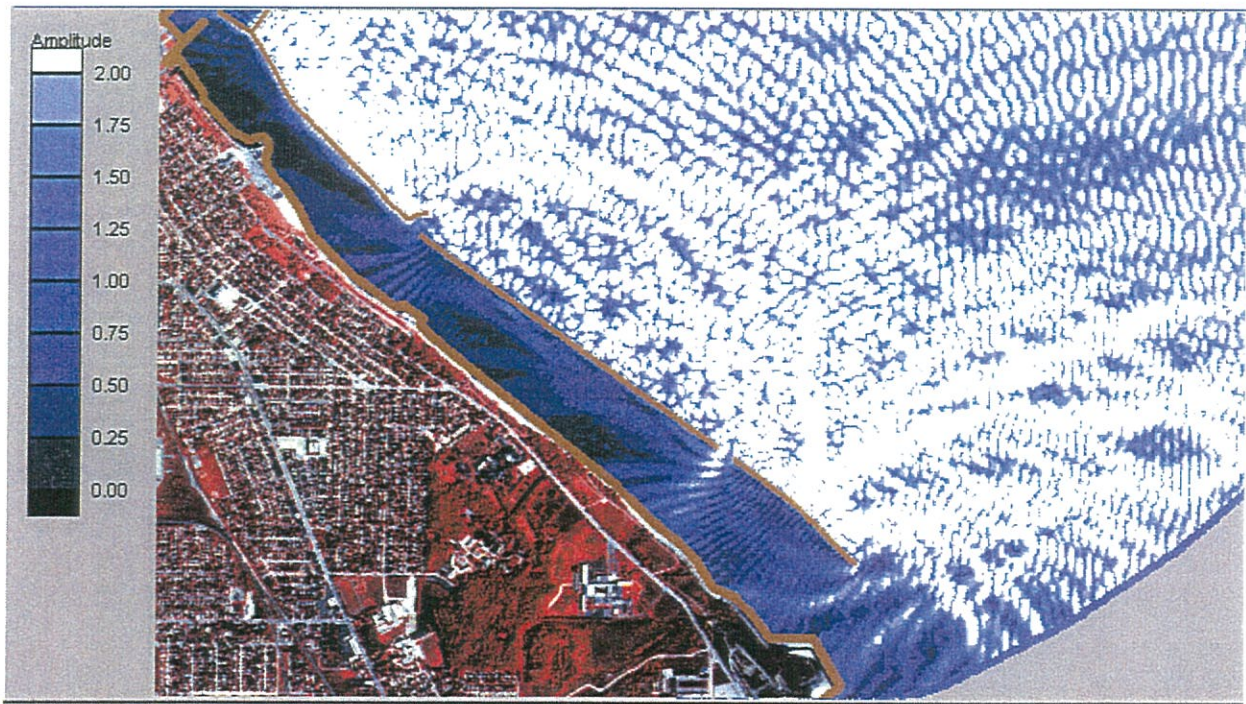


Figure A-18: Case 6 model output with 90 degree wave approach, 5m input wave-height and high SWE



Figure A-19: Case 7 model output with 160 degree wave approach, 5m input wave-height and high SWE



Figure A-20: Case 8 model output with 160 degree wave approach, 1m input wave-height and high SWE

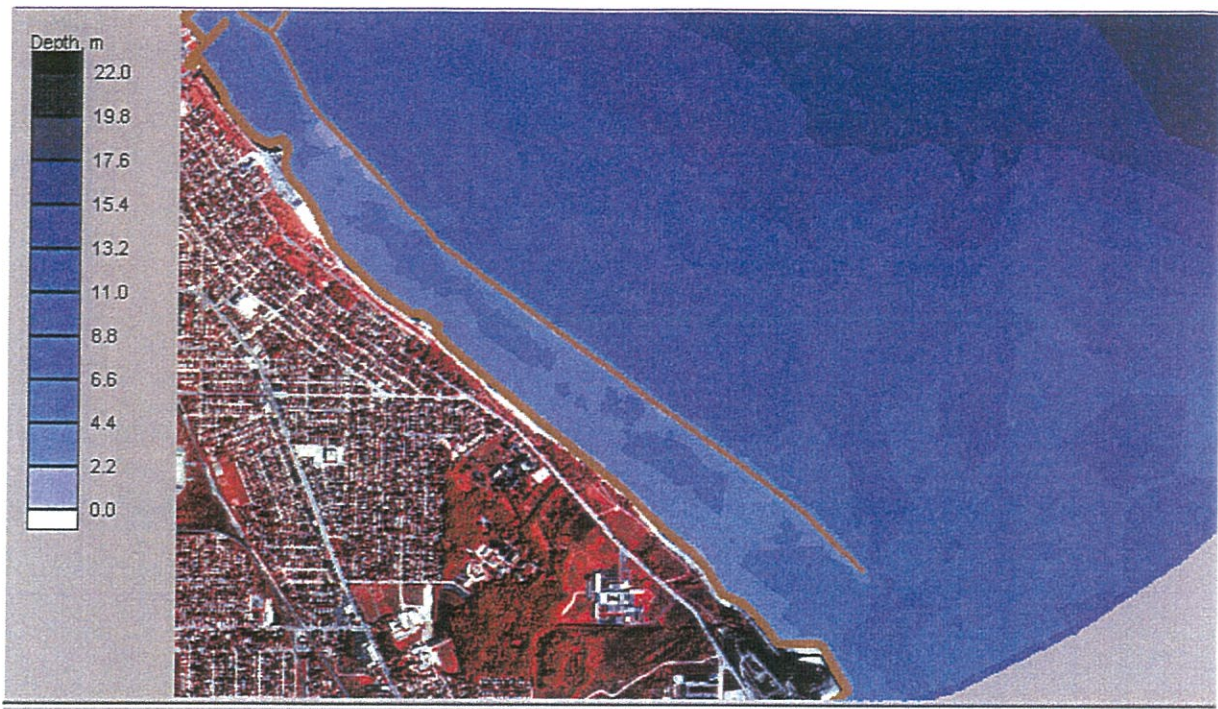


Figure A-21: Continuous breakwater configuration and bathymetry

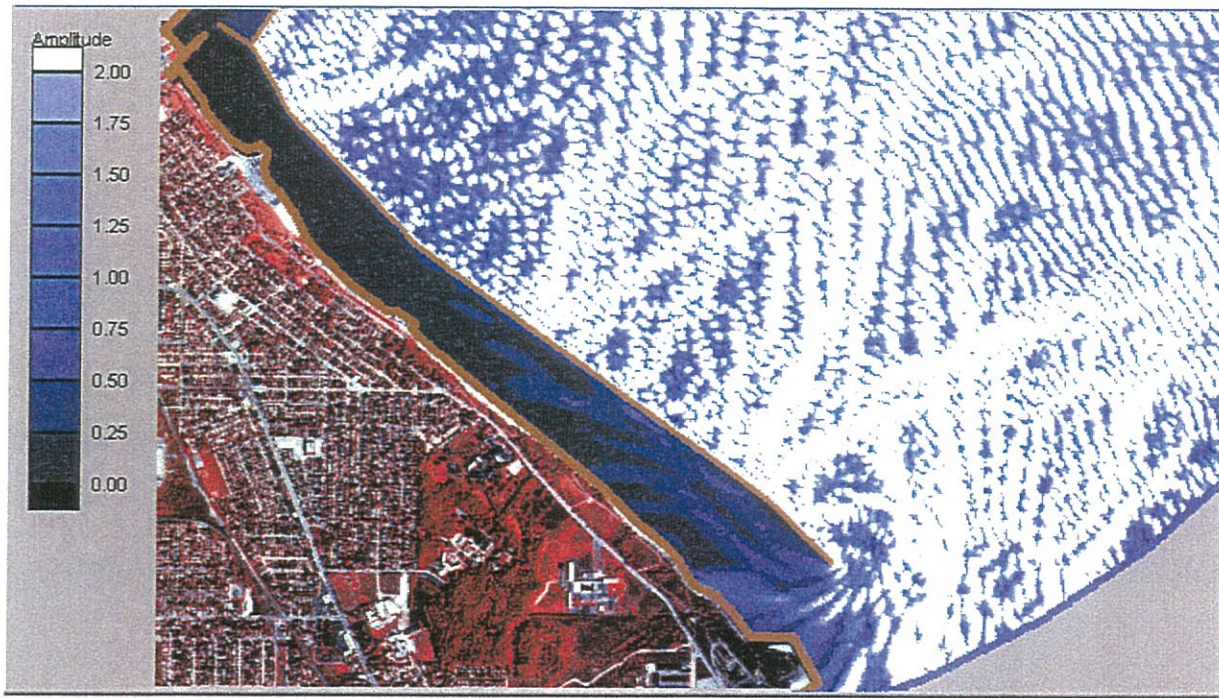


Figure A-22: Case 9 model output with 20 degree wave approach, 5m input wave-height and high SWE



Figure A-23: Case 10 model output with 160 degree wave approach, 5m input wave-height and high SWE



Figure A-24: No-breakwater configuration and bathymetry

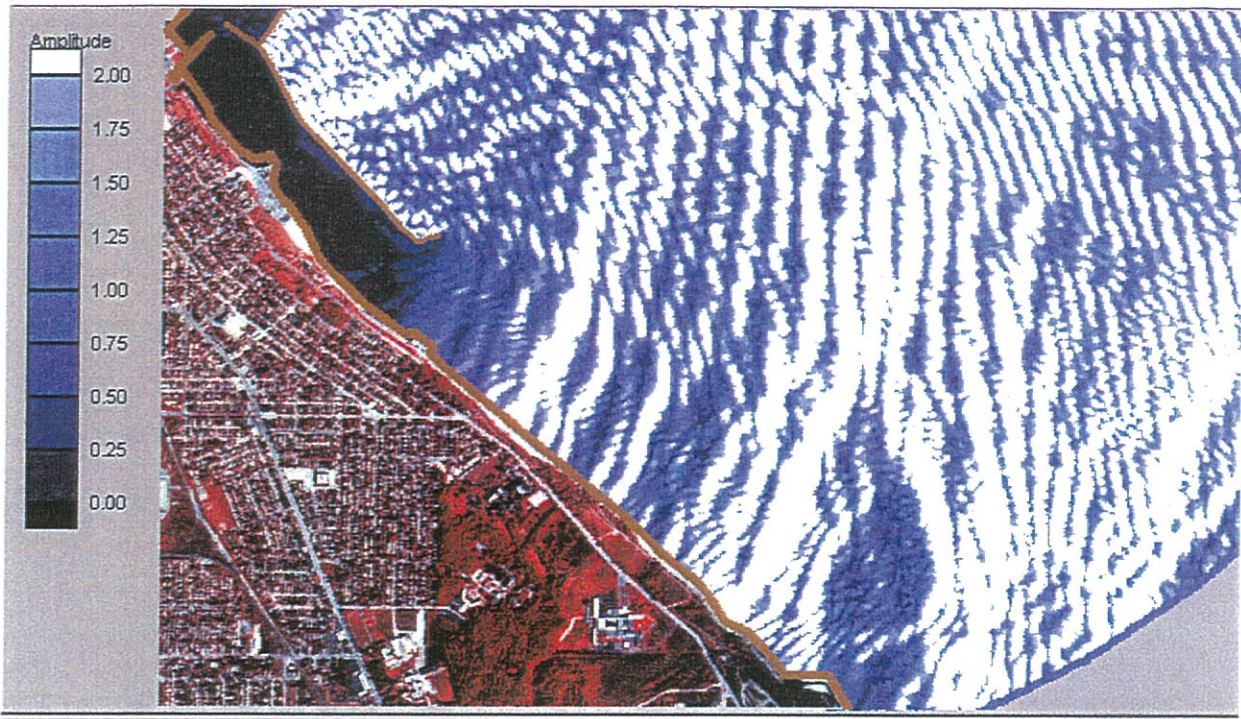


Figure A-25: Case 11 model output with 20 degree wave approach, 5m input wave-height and high SWE



Figure A-26: Case 12 model output with 160 degree wave approach, 5m input wave-height and high SWE

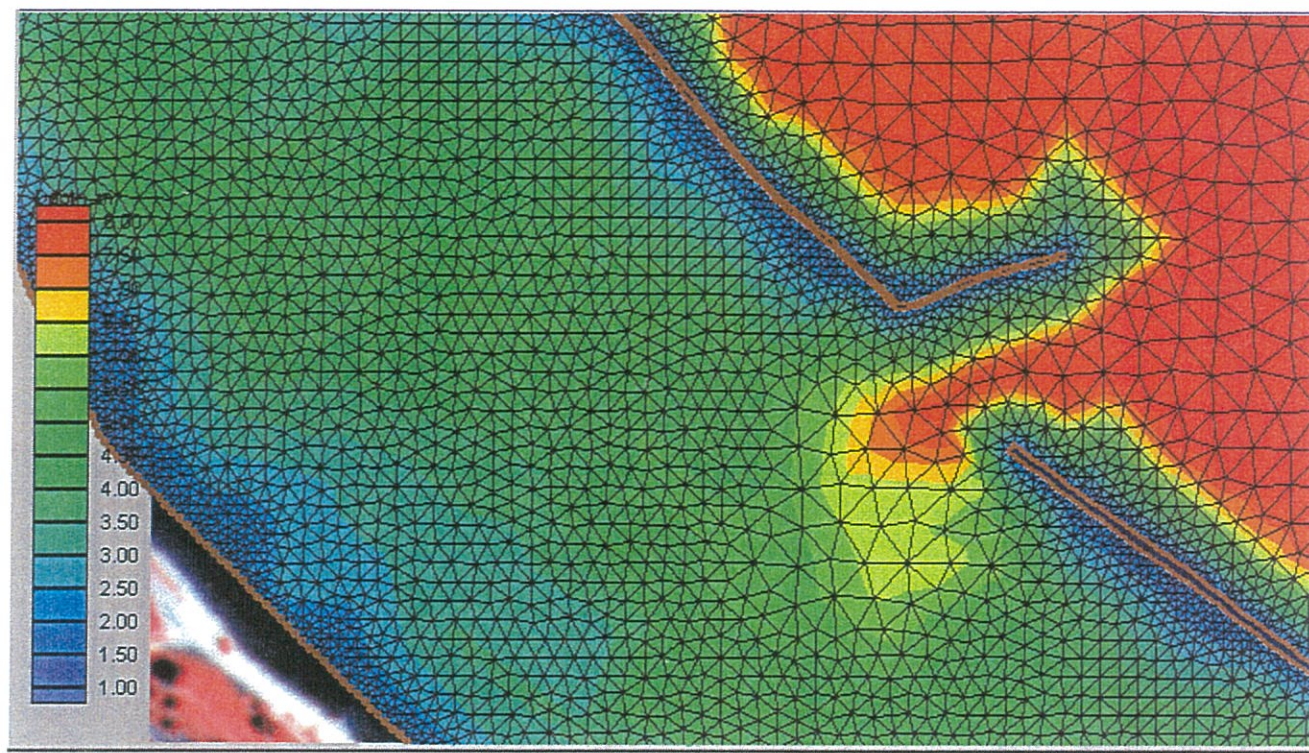


Figure A-27: Finite element grid and bathymetry at north opening

APPENDIX 2 - PHOTOGRAPHS



PHOTO #1: SHORELINE SOUTH OF SOUTH SHORE PARK, FACING NORTH. NOTE STONE PROTECTION AND GROINS..



PHOTO #2: SHORELINE FACING SOUTH, SOUTH OF SOUTH SHORE PARK. NOTE EROSION IN UNPROTECTED AREA.



PHOTO #3: SHORELINE COVERED WITH SMALL STONE HAS ERODED



PHOTO #4: SHORELINE FACING SOUTH – NOTICE STONE PROTECTION

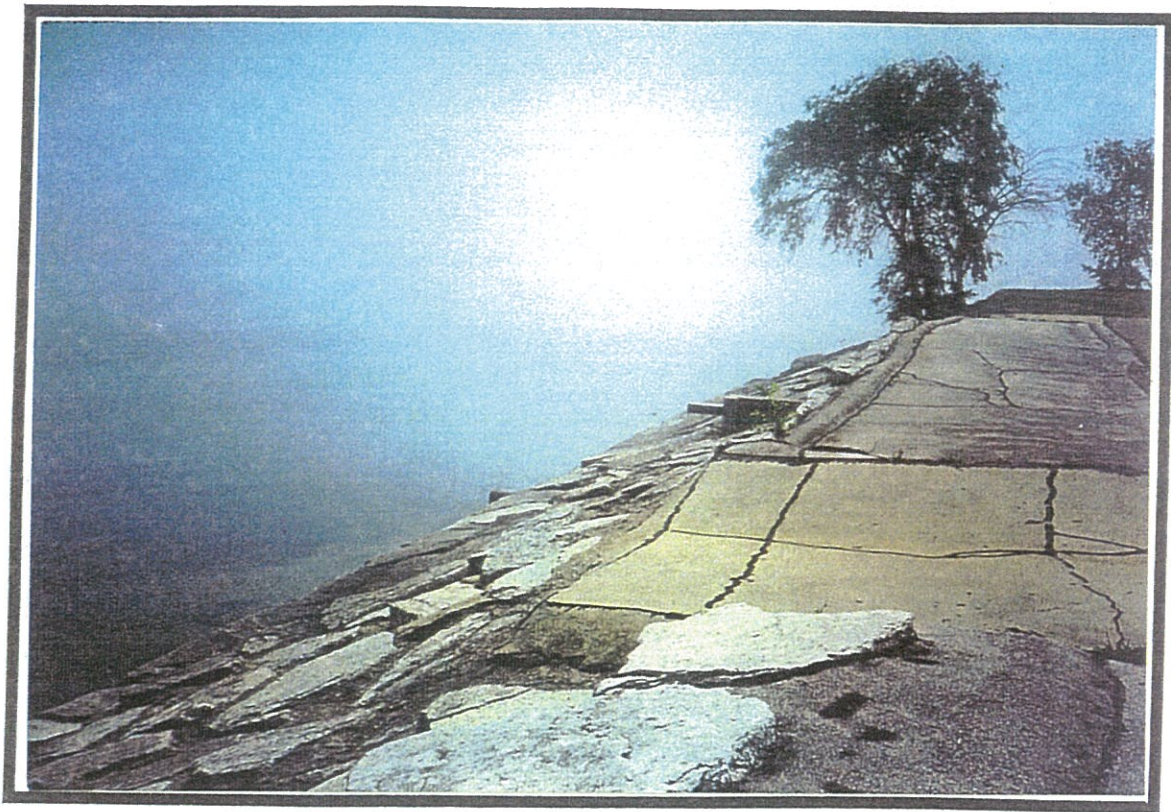


PHOTO #5: CONCRETE PROTECTION & FLAT STONES

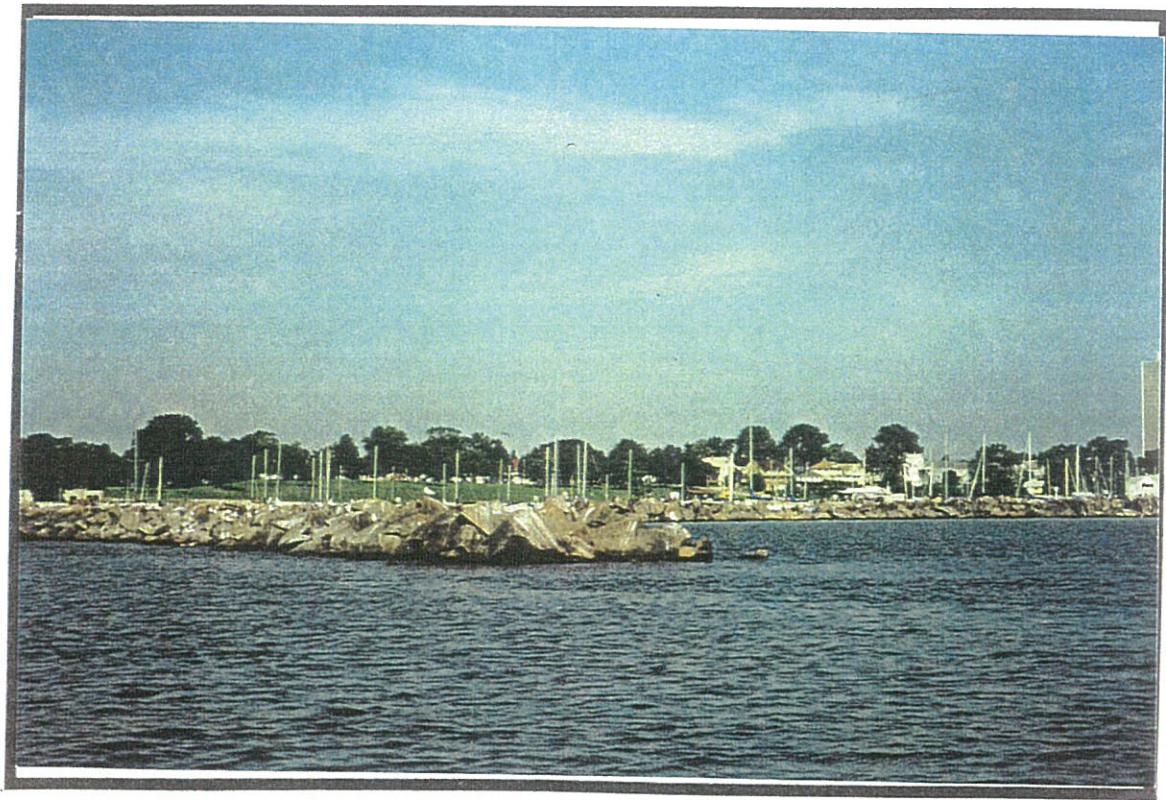


PHOTO #6: NORTH END OF BREAKWATER NEAR SOUTH SHORE PARK AND BOAT BASIN

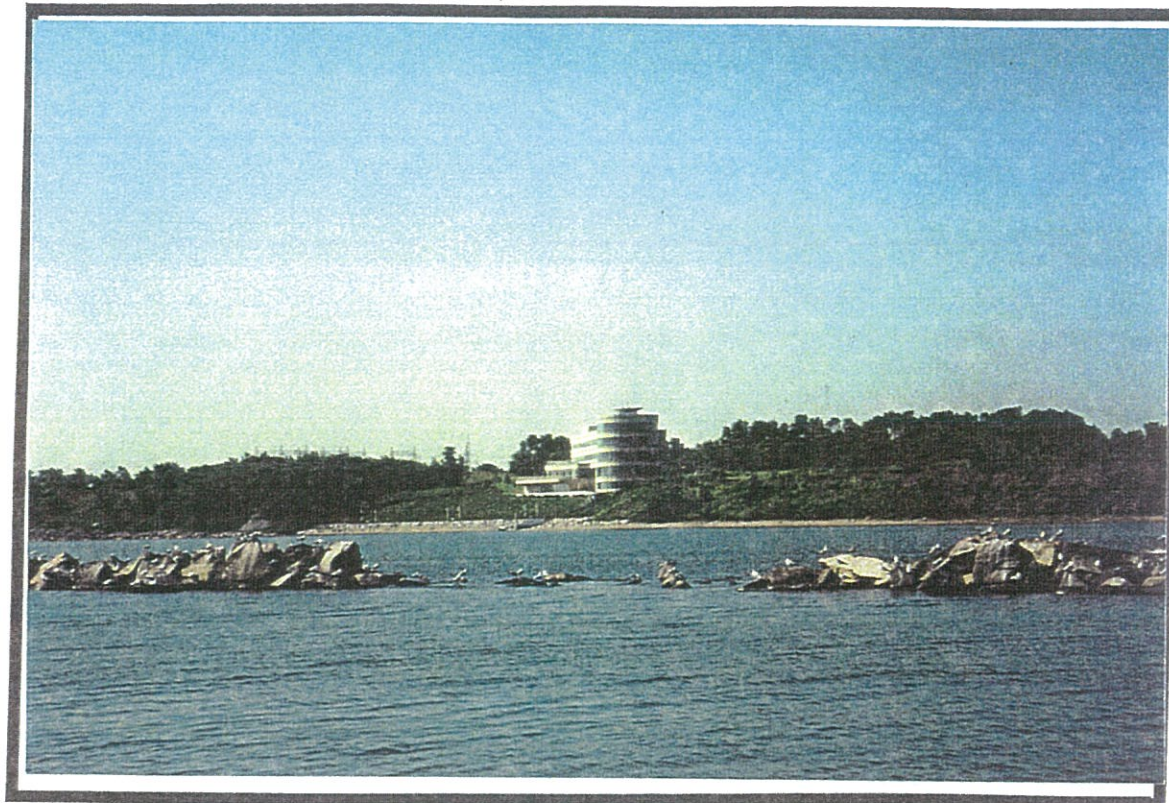


PHOTO #7: SOUTHERN END OF BREAKWATER



PHOTO #8: TYPICAL "GOOD" SECTION OF BREAKWATER. NOTE INTERLOCKING/
CHINKING OF STONE, ESTIMATED SIZE OF 7 TO 12 TONS.

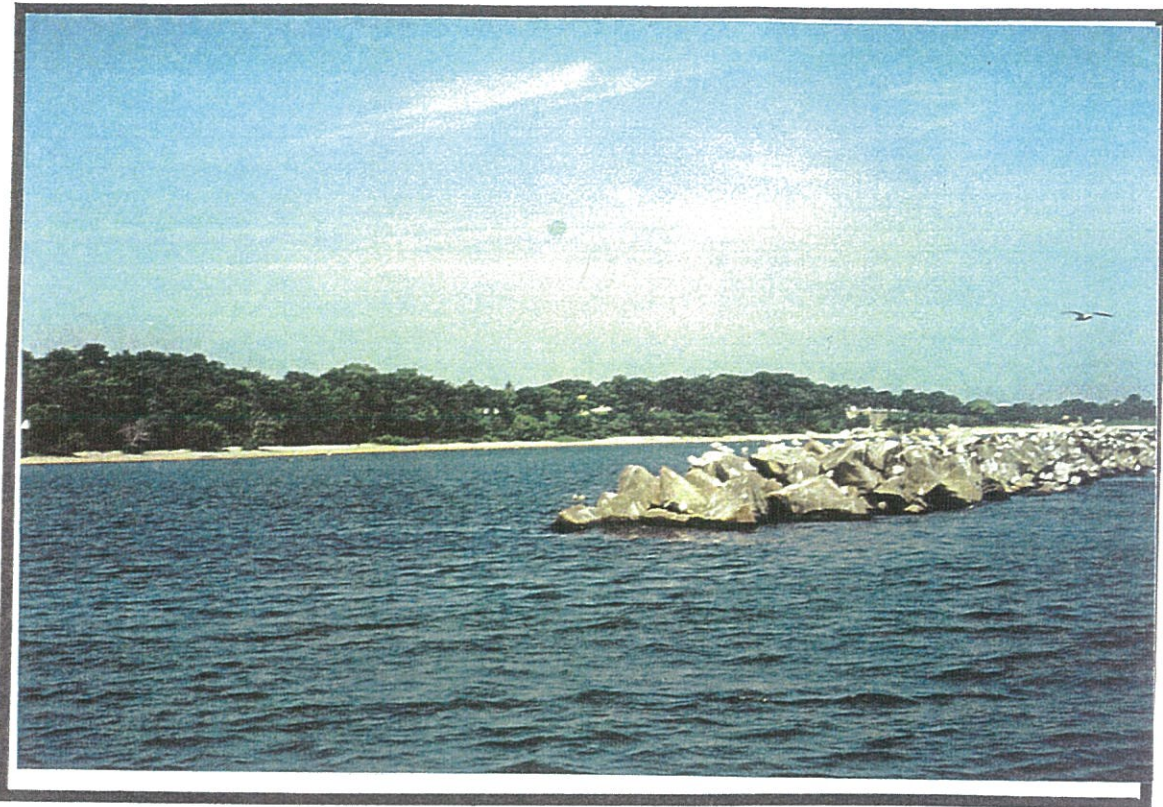


PHOTO #9: DESIGNED OPENING IN BREAKWATER – STONE FALLS OFF NEATLY/
UNIFORMLY TO THE WATER.



PHOTO #10: HOLE OR VOID IN BREAKWATER

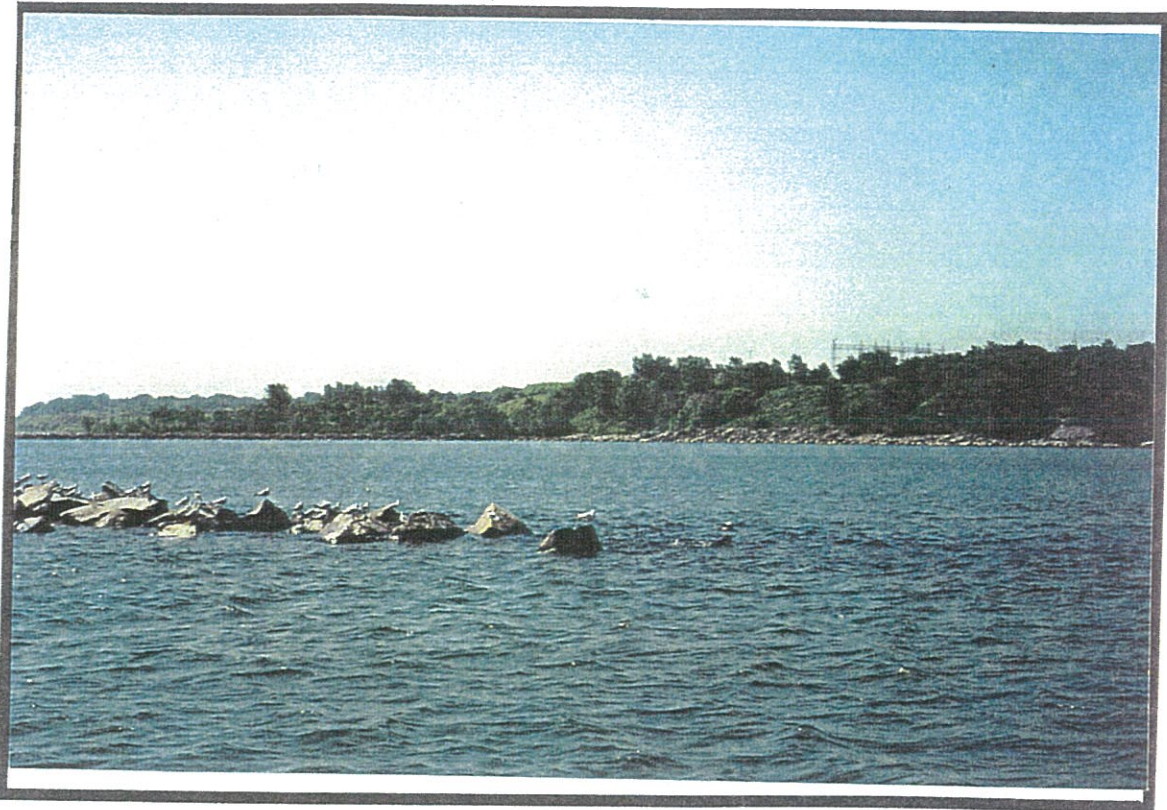


PHOTO #11: HOLE OR VOID IN BREAKWATER



PHOTO #12: VIEW OF BREAKWATER FROM SHORE



PHOTO #13: VIEW OF BREAKWATER FROM SHORELINE, NEAR SOUTHERN DESIGNED OPENING.



PHOTO #14: VIEW OF GROINS IN NORTHERN PROJECT AREA. NOTE DETERIORATION OF BREAKWATER.



PHOTO #15: LOOKING SOUTH ALONG SOUTHERN END OF BREAKWATER.



PHOTO #16: EXISTING STONE CONDITION, SOUTHERN END OF BREAKWATER.



PHOTO #17: GULLYING AT SOUTHERN END OF PROJECT AREA



PHOTO #18: GULLYING AT SOUTHERN END OF PROJECT AREA

APPENDIX 3 – COST ESTIMATE

